

Turbulent compressible fluid: Renormalization group analysis, scaling regimes, and anomalous scaling of advected scalar fields

N. V. Antonov^{1,*}, N. M. Gulitskiy^{1,†}, M. M. Kostenko^{1,‡} and T. Lučivjanský^{2,3§}

¹*Department of Physics, St. Petersburg State University,
7/9 Universitetskaya nab., St. Petersburg 199034, Russia*

²*Faculty of Sciences, P.J. Šafárik University, Moyzesova 16, 040 01 Košice, Slovakia*

³*Peoples' Friendship University of Russia (RUDN University),
6 Miklukho-Maklaya St., Moscow, 117198, Russia*

We study a model of fully developed turbulence of a compressible fluid, based on the stochastic Navier-Stokes equation, by means of the field theoretic renormalization group. In this approach, scaling properties are related to the fixed points of the renormalization group equations. Previous analysis of this model near the real-world space dimension 3 identified some scaling regime [Theor. Math. Phys., **110**, 3 (1997)]. The aim of the present paper is to explore the existence of additional regimes, that could not be found using the direct perturbative approach of the previous work, and to analyze the crossover between different regimes. It seems possible to determine them near the special value of space dimension 4 in the framework of double y and ε expansion, where y is the exponent associated with the random force and $\varepsilon = 4 - d$ is the deviation from the space dimension 4. Our calculations show that there exists an additional fixed point that governs scaling behavior. Turbulent advection of a passive scalar (density) field by this velocity ensemble is considered as well. We demonstrate that various correlation functions of the scalar field exhibit anomalous scaling behavior in the inertial-convective range. The corresponding anomalous exponents, identified as scaling dimensions of certain composite fields, can be systematically calculated as a series in y and ε . All calculations are performed in the leading one-loop approximation.

Keywords: anomalous scaling, passive scalar advection, turbulence, renormalization group

I. INTRODUCTION

Understanding fully developed turbulence is a complex, rich, and challenging problem. Among the most important features of such behavior are energy cascades and intermittency. The former brings energy from large scales, responsible for the creation of turbulence, into smaller ones, in which viscosity plays a major role and dissipation effects dominate. Intermittency, an irregular alternation of phases of certain dynamics, means that very rare configurations of a system contribute most significantly to statistical distributions. In turbulence this fact manifests itself in anomalous scaling, which is characterized by singular behavior of various statistical quantities as functions of the integral turbulence scales. Anomalous scaling is thought to be related to strong fluctuations of the energy flux and, therefore, to deviate from the predictions of the classical Kolmogorov-Obukhov phenomenological theory [1, 2].

Another very interesting phenomenon is a turbulent advection of an impurity field. Both experimental studies and numerical simulations suggest that deviations from the classical Kolmogorov theory are even more strongly pronounced for passively advected fields than for the velocity field itself [3–6]. A turbulent environment may be

introduced into such models by some “synthetic” velocity field with prescribed statistics or by the stochastic Navier-Stokes equation [7]. Models of the former type are more tractable from a mathematical point of view, whereas the latter ones bear a closer resemblance to the real world.

Fully developed turbulence is characterized by existence of an inertial range – an interval of scales in which both the input and dissipation of energy are insignificant, and the only notable dynamical process is the redistribution of energy along the spectrum. Therefore, one expects the inertial range to be governed by simple (and possibly universal) laws describing turbulent processes. In accordance with this hypothesis, the classical Kolmogorov-Obukhov theory assumes that statistical characteristics of a system, i.e., its correlation and response functions, do not depend on either the internal (l , viscosity-related) or the external (\mathcal{L} , external force-related) scales. These assumptions lead to simple power laws for inertial range asymptotic behavior of these functions [1, 2].

This notwithstanding, it is well known that correlation functions can depend on the external scale due to certain kinematic effects – for example, the sweeping effect, in which small turbulent eddies are carried by large ones as a whole without distortion. These kinematic effects do not influence the formation of the energy spectrum and, therefore, can be ignored in favor of Galilean invariant objects, in particular, equal-time correlation or structure functions. Nevertheless, experimental studies suggest that Galilean invariant objects also contain some dependence on \mathcal{L} , which is usually singular and is de-

* n.antonov@spbu.ru

† n.gulitskiy@spbu.ru

‡ kontramot@mail.ru

§ tomas.lucivjansky@upjs.sk

scribed by an infinite set of anomalous exponents – a phenomenon referred to as “anomalous scaling” and “multi-scaling.”

In many phenomenological models the anomalous exponents are related to the statistical properties of nonuniversal quantities such as the local dissipation rate, the characteristics of nontrivial structures (vortex filaments), and so on; see, e.g., [1, 2]. Common drawbacks of such models are that they are only loosely based on the underlying hydrodynamical equations, and they involve arbitrary adjustment parameters; therefore, these models cannot be used to construct systematic perturbation theory in a small expansion parameter [8].

Therefore, an essential goal of the theory of turbulence is to construct an analytic framework based on a dynamical model, e.g., the Navier-Stokes equation. The key obstacle in this situation is the lack of a small expansion parameter – at least, a formal one. In ordinary perturbation theory for the stochastic Navier-Stokes equation (i.e., expansion in the nonlinearity) the actual expansion parameter reduces to the Reynolds number, which tends to infinity for the developed turbulence.

A similar problem is longstanding in the theory of critical phenomena, where it was successfully solved by use of the renormalization group (RG) method borrowed from quantum field theory. The RG method performs a certain rearrangement (infinite resummation) of the original perturbation series, and turns them into a series of the parameter of order unity. Typically, that parameter is $\varepsilon = 4 - d$, the deviation of the dimensionality of space d from its upper critical value [9–14], hence the term “epsilon expansion.” Such expansions are still divergent, but they allow one to prove the existence of infrared (IR) scaling behavior (if such exists) and to systematically calculate the corresponding dimensions as series in ε .

The RG method and ε expansion are equally applicable to the stochastic Navier-Stokes equation if the correlation function of the random force is chosen as a power function of the momentum $k = |\mathbf{k}|$ in the form of k^{4-d-y} , see [14, 15] and Sec. II in the present paper. Here, d becomes a free parameter, while the role of the RG expansion parameter is played by the exponent y .

The results, obtained within the ε expansions, are reliable for asymptotically small values of ε , but it is unclear whether these results can be extrapolated to finite (and non-small) realistic values of ε . For this reason, in the theory of critical phenomena, one tries to calculate as many terms of the ε expansion as possible, to get their higher-order asymptotic form (using the instanton calculus) and to use additional methods of summation (for instance, Padé-Borel or Leroy-Borel transformations). A common opinion is that the ε expansion indeed works for real ε [9–11, 16].

For the Navier-Stokes turbulence, the situation is much more difficult. First, the RG expansion parameter y is not small, and the RG series are divergent. Second, the higher-order calculations are extremely cumbersome. Third, the higher-order asymptotic forms of the coeffi-

cients are not known yet. However, these problems can be considered as being of technical (calculational) nature. There are more serious problems, specific only for turbulence, which are related to real physical effects: sweeping of small turbulent eddies by large-scale ones, and the anomalous scaling. In perturbation theory both of them manifest as strong divergences of the perturbation diagrams at $\mathcal{L} \rightarrow \infty$ (where \mathcal{L} is the integral, i.e., external, turbulence scale) in the inertial range. Adequate analysis of these issues takes one far beyond the standard RG method: the method should be combined with the short-distance operator product expansion (OPE).

The feature specific of the models of turbulence is the existence in the corresponding OPE of composite fields (“operators” in quantum field terminology) with negative critical dimensions. These operators (termed “dangerous”) give rise to strong IR singularities in the correlation functions; see [9, 14, 17–19]. While experimental data suggests that in the inertial range correlation and structure functions exhibit anomalous scaling, it has not been possible to demonstrate this property through theoretical modeling. The main problem is the following: if a dangerous operator is present in some field theory there are, in fact, infinitely many such operators; moreover, the spectrum of these operators is not bound from below. Thus, there is no main, or “most dangerous,” operator in the model that would provide the main contribution in the corresponding OPE; see, e.g., Appendix A in [20]. Therefore, the problem requires one to perform the explicit construction of all invariant scalar operators with negative dimensions, the exact calculation of their critical dimensions, and the (infinite) summation of their contributions in the corresponding OPE.

Clearly, there is little hope to solve this problem in the foreseeable future. Fortunately, situation simplifies for two important cases: sweeping effects and passive advection. The first example is provided by the composite operators, which are powers of the velocity field in the stochastic Navier-Stokes equation. Owing to the Galilean symmetry of the model, their dimensions can be found exactly, and their contributions into the OPE can be summed up into an explicit closed expression [9, 14, 18, 19]. This gives adequate description of the sweeping effects within the RG+OPE approach.

The second case is provided by the passive advection of scalar or vector fields by a given velocity statistics. The stochastic advection-diffusion equation is linear in these fields, therefore, only finite number of dangerous operators contribute to the OPE for any given correlation function, and the additional resummation of the series, discussed above, is not required [21]. Therefore, one way to investigate these phenomena is to consider a passive advection of different types of fields by successively more complex and realistic turbulent velocity environments. In a number of papers the RG+OPE approach has been applied to passive advection by Kraichnan’s ensemble (the velocity field is assumed to be isotropic, Gaussian, not correlated in time, and to have a power-like corre-

lation function; the fluid is assumed to be incompressible) [15, 21–23], and by the ensemble’s numerous generalizations: large-scale anisotropy, helicity, compressibility, finite correlation time, non-Gaussianity, and a more general form of nonlinearity [24–35]. This approach can be generalized to a non-Gaussian velocity field governed by the stochastic Navier-Stokes equation, to study both the velocity field’s scaling behavior and passive impurity fields it advects [20, 36–40]. The main advantage of the RG+OPE approach as applied to turbulence is that it is based on a microscopic model and, therefore, allows one to construct a systematic perturbation expansion for the anomalous exponents.

Until now, the majority of studies on fully developed turbulence have been concerned with incompressible fluid. Nevertheless, several results for the problems of universality and scaling for compressible fluids have also been obtained [41–51]. All of them hint at large influence of compressibility both on the velocity field itself and on passively advected quantities. In particular, a transition from a turbulent to a certain purely chaotic state may occur at large degrees of compressibility [46]. In other papers corrections in the Mach number to the incompressible scaling regime were studied [52–54]. The main result of those studies is that obtained corrections become arbitrarily large and destroy the incompressible scaling regime for fixed Mach numbers and large distances, what can be explained by existence of a crossover to another, yet unknown regime. The studies [55–57] were devoted to compressible fluids. The results are rather controversial; particularly, the model, considered in [56], appears to be non-renormalizable. From a general point of view, further investigations of compressibility are therefore called for.

In this paper we present an application of the field theoretic renormalization group to the scaling regimes of a compressible fluid whose behavior is governed by a proper generalization of the stochastic Navier-Stokes equation [55]. The stationary scaling regimes in this approach are associated with IR attractive fixed points of the corresponding multiplicatively renormalizable field theoretic models. One nontrivial fixed point for this model, attractive in our region of interest, was found in [55]. In [20, 38] the scaling properties of passively advected scalar and vector fields by this velocity ensemble were investigated and anomalous scaling for different correlation functions was discovered.

The analysis in [55] and subsequent papers [20, 38] is self-contained and internally consistent for asymptotically small y , where y describes the scaling behavior of a random force [see (2.8)]. However, as y grows some effects can happen: the fixed point, found within the analysis at small y , can lose its stability or go to unphysical region. In the same time, another fixed point(s), which are not “visible” within the y -expansion, may begin to determine the IR behaviour. Therefore, it is feasible that other fixed points (and other scaling regimes with other critical dimensions) exist for finite (non-small) values of

y . These fixed points cannot be identified within the frameworks of the analysis at small y and in this sense are non-perturbative. However, some of them can be revealed in a double expansion in y and the deviation from the space dimension d from some exceptional values, like $d = 2$ for the incompressible case [58–60]. Indeed, for the incompressible case, the double expansion in y and $(d - 2)$ reveals two non-trivial fixed points (and hence two asymptotic regimes), one corresponding to the equilibrium (thermal) regime [61] and the other to the turbulence [14, 58].

In the compressible case there are also two special dimensions, namely $d = 2$ and $d = 4$, in which the renormalization procedure is much more complicated in comparison to all other situations. The double expansion around $d = 2$ is currently under consideration [62]; $d = 4$ admits the double expansion in y and $\varepsilon = (4 - d)$ and is employed in the present paper. Model analysis near this special dimension allows us to not only extend previous research [38, 55] (by refining the known scaling regimes through resummation of the ordinary y expansion), but also to investigate the existence of other possible regimes. This is the main subject and motivation of the present study. We show that a new fixed point (henceforth called “local” for the reasons to be explained) indeed exists near $d = 4$ and persists, at least in the leading one-loop approximation, for all d . The other “non-local” fixed point corresponds to the scaling regime found earlier [55]. The regions of stability and critical dimensions for both fixed points are calculated in the leading one-loop order.

Following the procedure of previous studies [38, 55, 63], first the stochastic Navier-Stokes equation is discussed. After establishing the existence of necessary fixed points of Navier-Stokes equation, the advection of scalar fields is explored. Since RG functions of the parameters, entering the Navier-Stokes equation do not depend on the parameters, connected with advection-diffusion equation, this is a possible and probably the easiest approach.

The paper is organized as follows:

In Sec. II, a detailed description of the stochastic Navier-Stokes equation for a compressible fluid is given. Sec. III is devoted to field theoretic formulation of the model and the corresponding diagrammatic technique. In particular, possible types of divergent Green functions at $d = 3$ and $d = 4$ and the necessity of introducing a new coupling constant at $d = 4$ are discussed. In Sec. IV, the renormalizability of the model is established and one-loop explicit expressions for the renormalization constants and RG functions (anomalous dimensions and β functions) are derived. In Sec. V, the obtained expressions for RG functions are examined. IR asymptotic behavior, obtained by solving the RG equations, is discussed. It is shown that, depending on two exponents y and ε , the RG equations possess an IR attractive fixed point, which implies existence of a scaling regime in the inertial range. The corresponding scaling dimensions of all fields and parameters of the model are presented.

In Sec. VI, an advection of a passive scalar (density) field by compressible velocity field which obeys Navier-Stokes equation is analyzed. A field theoretic formulation of the full model is presented. It is shown that the full model is multiplicatively renormalizable; the existence of a scaling regime in the IR range is established. The renormalization of composite operators is carried out. An inertial-range behavior of various correlation functions is studied by means of the OPE. It is shown that leading terms of the inertial-range behavior are determined by the contributions of the operators built solely from the scalar fields. As a result, the IR behavior of the pair correlation functions of the composite operators is power-like with negative critical dimensions – a situation, called anomalous scaling.

Sec. VII is reserved for conclusions. The main one is that the new (local) fixed point indeed exists in the model of turbulence for a compressible fluid, based on the stochastic Navier-Stokes equation.

Appendices A and B contain detailed calculations of all diagrams, needed to perform multiplicative renormalization of our model.

II. DESCRIPTION OF THE MODEL

The Navier-Stokes equation for a viscous compressible fluid can be written in the following form [64]:

$$\rho \nabla_t v_i = \nu_0 (\delta_{ik} \partial^2 - \partial_i \partial_k) v_k + \mu_0 \partial_i \partial_k v_k - \partial_i p + \eta_i, \quad (2.1)$$

where the differential operator in the right hand side

$$\nabla_t = \partial_t + v_k \partial_k \quad (2.2)$$

is the Lagrangian (convective) derivative, ρ is a fluid density field, v_i is the velocity field, $\partial_t = \partial/\partial t$, $\partial_i = \partial/\partial x_i$, $\partial^2 = \partial_i \partial_i$ is the Laplace operator, p is the pressure field, and η_i is the density of an external force per unit volume. The fields v_i , η_i , ρ and p depend on $x = (t, \mathbf{x})$ with $\mathbf{x} = (x_1, x_2, \dots, x_d)$, where d is the dimensionality of space. The constants ν_0 and μ_0 are two independent molecular viscosity coefficients [64]; in (2.1) we have explicitly separated the transverse and longitudinal components of the viscous term. Summations over repeated vector indices are always implied in this work.

To get a closed system of equations, the model (2.1) must be augmented by two additional equations, namely a continuity equation and an equation of state between deviations δp and $\delta \rho$ from the equilibrium values. They explicitly read

$$\partial_t \rho + \partial_i (\rho v_i) = 0 \quad (2.3)$$

and

$$\delta p = c_0^2 \delta \rho. \quad (2.4)$$

In order to derive renormalizable field theory, the stochastic equation (2.1) has to be divided by ρ , and fluctuations in viscous terms have to be neglected [54]. Further, by using the expressions (2.3) and (2.4) the problem can be recast in the form of two coupled equations:

$$\begin{aligned} \nabla_t v_i &= \nu_0 (\delta_{ik} \partial^2 - \partial_i \partial_k) v_k + \mu_0 \partial_i \partial_k v_k - \partial_i \phi + f_i, \\ \nabla_t \phi &= -c_0^2 \partial_i v_i. \end{aligned} \quad (2.5)$$

Here, a new scalar field $\phi = \phi(x)$ is related to the density fluctuations via the relation $\phi = c_0^2 \ln(\rho/\bar{\rho})$. A parameter c_0 is the adiabatic speed of sound, $\bar{\rho}$ denotes the mean value of ρ , and $f_i = f_i(x)$ is a density of the external force per unit mass.

In the stochastic formulation of the problem the turbulence is modeled by an external force – it is assumed to be a random variable, which mimics the input of energy into the system from the outer large scale \mathcal{L} . Its precise form is believed to be unimportant and is usually considered to be a random Gaussian variable with zero mean and prescribed correlation function [9]. For the use of the standard RG technique this correlator must exhibit a power law asymptotic behavior at large wave numbers [14, 65]. In the case of compressible fluid it should be naturally augmented with a longitudinal component, hence, the simplest way is to choose it in the form [55]

$$\langle f_i(t, \mathbf{x}) f_j(t', \mathbf{x}') \rangle = \frac{\delta(t-t')}{(2\pi)^d} \int_{k>m} d^d \mathbf{k} \tilde{D}_{ij}(\mathbf{k}) e^{i\mathbf{k} \cdot (\mathbf{x} - \mathbf{x}')}, \quad (2.7)$$

where the argument is given by

$$\tilde{D}_{ij}(\mathbf{k}) = g_{10} \nu_0^3 k^{4-d-y} \left\{ P_{ij}(\mathbf{k}) + \alpha Q_{ij}(\mathbf{k}) \right\}. \quad (2.8)$$

Here, $P_{ij}(\mathbf{k}) = \delta_{ij} - k_i k_j / k^2$ and $Q_{ij}(\mathbf{k}) = k_i k_j / k^2$ are the transverse and longitudinal projectors, $k = |\mathbf{k}|$, the amplitude α is a free parameter, the amplitude g_{10} is a coupling constant (formal expansion parameter in the ordinary perturbation theory); the relation $g_{10} \sim \Lambda^y$ sets in the typical ultraviolet (UV) momentum scale Λ , which is a reciprocal of the dissipation length scale. A parameter $m = \mathcal{L}^{-1}$ provides an infrared regularization; its precise form is unessential and the sharp cut-off is the simplest choice for calculation purposes. The exponent y provides analytic UV regularization and, therefore, plays a role of a formally small expansion parameter [9]. The most realistic (physical) value is obtained in the limit $y \rightarrow 4$, when the function in (2.8) can be interpreted as power-like representation of the Dirac function $\delta(\mathbf{k})$: physically it corresponds to the idealized picture of the energy input from infinitely large scales. The Galilean invariance for the model (2.1) is ensured when the function (2.8) is delta-correlated in time [14].

III. FIELD THEORETIC FORMULATION OF THE MODEL

A. Action functional and Feynman rules

According to the general theorem [9, 10], the stochastic problem (2.5) – (2.8) is equivalent to the field theoretic model with a doubled set of fields $\Phi = \{v_i, v'_i, \phi, \phi'\}$ and De Dominicis-Janssen action functional, written in a compact form as

$$\begin{aligned} \mathcal{S}_v(\Phi) = & \frac{v'_i \tilde{D}_{ij} v'_j}{2} + v'_i \left[-\nabla_t v_i + \nu_0 (\delta_{ij} \partial^2 - \partial_i \partial_j) v_j + u_0 \nu_0 \partial_i \partial_j v_j - \partial_i \phi \right] \\ & + \phi' [-\nabla_t \phi + \nu_0 \nu_0 \partial^2 \phi - c_0^2 (\partial_i v_i)], \end{aligned} \quad (3.1)$$

where \tilde{D}_{ij} is the correlation function (2.8). Here we employ a condensed notation, in which integrals over the spatial variable \mathbf{x} and the time variable t , as well as summation over repeated indices, are implicitly assumed, i.e.,

$$\phi' \partial_t \phi = \int dt \int d^d \mathbf{x} \phi'(t, \mathbf{x}) \partial_t \phi(t, \mathbf{x}); \quad (3.2)$$

$$v'_i D_{ik} v'_k = \int dt \int d^d \mathbf{x} \int d^d \mathbf{x}' v'_i(t, \mathbf{x}) D_{ik}(\mathbf{x} - \mathbf{x}') v'_k(t, \mathbf{x}').$$

Moreover, we have introduced a new dimensionless parameter $u_0 = \mu_0/\nu_0 > 0$ and a new term $\nu_0 \nu_0 \phi' \partial^2 \phi$ with another positive dimensionless parameter ν_0 , which is needed to ensure multiplicative renormalizability. The action (3.1) is amenable to the standard methods of the quantum field theory, such as Feynman diagrammatic technique and renormalization group procedure.

In the standard field theoretic approach to the stochastic Navier-Stokes equation, the actual RG expansion parameter is y , while d plays a passive role; see the monographs [9, 14] for details. Our approach closely follows the analysis of the incompressible Navier-Stokes equation near space dimension $d = 2$ [58–60]. In this case an additional UV divergence appears in the Green function $\langle v'_i v'_j \rangle$. It can be absorbed by a suitable local counterterm $v'_i \partial^2 v'_i$, and a regular expansion in both y and $\varepsilon' = d - 2$ must be constructed. Up to now the present model (3.1) has been investigated in fixed space dimension $d = 3$, for which the action (3.1) contains all terms that can be generated during the renormalization procedure [20, 38, 55]. However, from the dimensional analysis (see below) it follows that in $d = 4$ an additional divergence appears in a similar fashion in the Green function $\langle v'_i v'_j \rangle$. Therefore, to keep the model renormalizable in $d = 4$, the kernel function $\tilde{D}_{ij}(\mathbf{k})$ in (2.7) has to be replaced by $D_{ij}(\mathbf{k})$, where

$$D_{ij}(\mathbf{k}) = g_{10} \nu_0^3 k^{4-d-y} \left\{ P_{ij}(\mathbf{k}) + \alpha Q_{ij}(\mathbf{k}) \right\} + g_{20} \nu_0^3 \delta_{ij}. \quad (3.3)$$

A new term on the right hand side with an additional coupling constant g_{20} absorbs divergent contributions from $\langle v'_i v'_j \rangle$. In contrast to the two-dimensional incompressible case [58] no momentum dependence is needed here.

The field theoretic formulation (3.1) means that various correlation and response functions of the original stochastic problem are represented by functional averages over the full set of fields with the functional weight $\exp \mathcal{S}(\Phi)$, and in this sense they can be viewed as Green functions of the field theoretic model [9, 10].

The perturbation theory of the model can be constructed according to the usual Feynman diagrammatic expansion [9, 10]. Bare propagators are read off from the inverse matrix of the Gaussian (free) part of the action functional, while a nonlinear part of the differential equation determines the interaction vertices. A graphical representation of the propagator functions is depicted in Fig. 1, and of the vertices – in Fig. 2. From (3.1) it follows that the Feynman diagrammatic technique for this model contains two interactions, $-v'_i (v_j \partial_j) v_i$ and $-\phi' (v_i \partial_i) \phi$. The propagator functions in the frequency-momentum representation read

$$\begin{aligned} \langle v_i v'_j \rangle_0 &= \overline{\langle v'_j v_i \rangle_0} = P_{ij}(\mathbf{k}) \epsilon_1^{-1} + Q_{ij}(\mathbf{k}) \epsilon_3 R^{-1}, \\ \langle v_i v_j \rangle_0 &= P_{ij}(\mathbf{k}) \frac{d_1^f}{|\epsilon_1|^2} + Q_{ij}(\mathbf{k}) d_2^f \left| \frac{\epsilon_3}{R} \right|^2, \\ \langle \phi v'_j \rangle_0 &= \overline{\langle v'_j \phi \rangle_0} = -\frac{ic_0^2 k_j}{R}, \quad \langle v_i \phi' \rangle_0 = \overline{\langle \phi' v_i \rangle_0} = -\frac{ik_i}{R}, \\ \langle \phi \phi' \rangle_0 &= \overline{\langle \phi' \phi \rangle_0} = \frac{\epsilon_2}{R}, \quad \langle \phi \phi \rangle_0 = \frac{c_0^4 k^2 d_2^f}{|R|^2}, \\ \langle v_i \phi \rangle_0 &= \overline{\langle \phi v_i \rangle_0} = \frac{ic_0^2 d_2^f \epsilon_3 k_i}{|R|^2}, \\ \langle \phi' \phi' \rangle_0 &= \langle v'_i \phi' \rangle_0 = \langle v'_i v'_j \rangle_0 = 0, \end{aligned} \quad (3.4)$$

where the symbol \bar{z} denotes the complex conjugate of the expression z . For convenience, the following abbreviations have been used

$$\begin{aligned} \epsilon_1 &= -i\omega + \nu_0 k^2, & \epsilon_2 &= -i\omega + u_0 \nu_0 k^2, \\ \epsilon_3 &= -i\omega + \nu_0 \nu_0 k^2, & R &= \epsilon_2 \epsilon_3 + c_0^2 k^2 \end{aligned} \quad (3.5)$$

and

$$\begin{aligned} d_1^f &= g_{10} \nu_0^3 k^{4-d-y} + g_{20} \nu_0^3, \\ d_2^f &= \alpha g_{10} \nu_0^3 k^{4-d-y} + g_{20} \nu_0^3. \end{aligned} \quad (3.6)$$

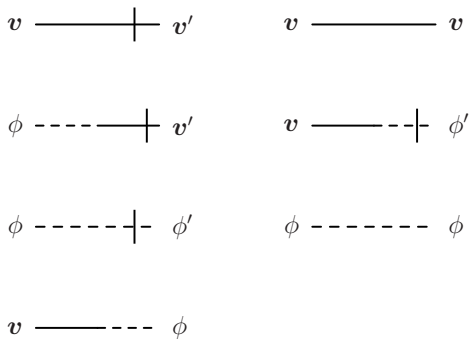


FIG. 1. Graphical representation of the bare propagators in the model (3.1).

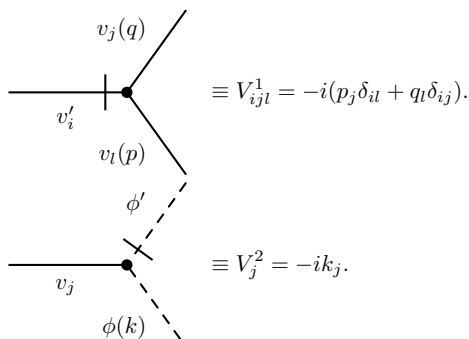


FIG. 2. Graphical representation of the interaction vertices in the model (3.1).

In the limit $c_0 \rightarrow \infty$ the propagator functions $\langle v_i v_j \rangle_0$ and $\langle v_i v'_j \rangle_0$ become purely transverse, and all the mixed propagators except $\langle \phi v'_j \rangle_0$ vanish. Moreover, the scalar fields ϕ and ϕ' decouple from the velocity fields v_i and v'_i – it is impossible to construct a diagram with only velocity fields v_i and v'_i as external lines, containing internal lines with fields ϕ or ϕ' . Thus, in conformity with the physical point of view, the well-known Feynman rules for the incompressible fluid [9, 14] are obtained.

From here on, a solid line without a slash denotes the field v_i , a solid line with a slash corresponds to the field v'_i , a dashed line without a slash denotes the field ϕ , and a dashed line with a slash corresponds to the field ϕ' .

B. Canonical dimensions, UV divergences, and renormalization constants

Ultraviolet renormalizability is very efficiently exhibited in analysis of the 1-particle irreducible Green functions, later referred to as 1-irreducible Green functions following the notation in [9]. In the case of dynamical models [9, 12] two independent scales have to be introduced: the time scale T and the length scale L . Thus the canonical dimension of any quantity F (a field or a parameter) is described by two numbers, the frequency dimension d_F^ω and the momentum dimension d_F^k , defined

such that

$$\begin{aligned} d_k^k &= -d_x^k = 1, & d_\omega^\omega &= d_x^\omega = 0, \\ d_\omega^\omega &= -d_t^\omega = 1, & d_\omega^k &= d_t^k = 0, \end{aligned} \quad (3.7)$$

i.e.,

$$[F] \sim [T]^{-d_F^\omega} [L]^{-d_F^k}. \quad (3.8)$$

The remaining dimensions can be found from the requirement that each term of the action functional be dimensionless, with respect to the momentum and the frequency dimensions separately.

Based on d_F^k and d_F^ω the total canonical dimension $d_F = d_F^k + 2d_F^\omega$ can be introduced, which in the renormalization theory of dynamic models plays the same role as the conventional (momentum) dimension does in static problems. Setting $\omega \sim k^2$ ensures that all the viscosity and diffusion coefficients in the model are dimensionless. Another option is to set the speed of sound c_0 dimensionless and consequently obtain that $\omega \sim k$, i.e., $d_F = d_F^k + d_F^\omega$. This variant would mean that we are interested in the asymptotic behavior of the Green functions as $\omega \sim k \rightarrow 0$, in other words, in sound modes in turbulent medium. Even though this problem is very interesting itself, it is not yet accessible for the RG treatment, so we will not discuss it here. The choice $\omega \sim k^2 \rightarrow 0$ is the same as in the models of incompressible fluid, where it is the only possibility because the speed of sound is infinite. A similar alternative in dispersion laws exists, for example, within the so-called model H of equilibrium dynamical critical behavior, see [9, 12].

The canonical dimensions for the model (3.1) are listed in Table I, including renormalized parameters (without the subscript “0”) and scalar impurity fields θ and θ' and parameter w , which appears in Sec. VI. From Table I it follows that the model is logarithmic (the coupling constants $g_{10} \sim [L]^{-y}$ and $g_{20} \sim [L]^{-\varepsilon}$ become dimensionless) at $y = \varepsilon = 0$. In this work we use the minimal subtraction (MS) scheme for the calculation of renormalization constants. In this scheme the UV divergences in the Green functions manifest themselves as poles in y, ε and their linear combinations. Here, in accordance with critical phenomena we retain the notation $\varepsilon = 4 - d$.

The total canonical dimension of any 1-irreducible Green function Γ is expressed by the relation

$$\delta_\Gamma = d + 2 - \sum_{\Phi} N_\Phi d_\Phi, \quad (3.9)$$

where N_Φ is the number of the given type of field entering the function Γ , d_Φ is the corresponding total canonical dimension of field Φ , and the summation runs over all types of the fields Φ in function Γ [9, 10, 12].

Superficial UV divergences whose removal requires counterterms can be present only in those functions Γ for which the formal index of divergence δ_Γ is a non-negative integer. Dimensional analysis should be augmented by the following additional considerations:

TABLE I. Canonical dimensions of the fields and parameters.

F	v'_i	v_i	ϕ'	ϕ	θ'	θ	m, μ, Λ	$\nu_0, \nu, \kappa, \kappa_0$	c_0, c	g_{10}	g_{20}	$u_0, v_0, w_0, u, v, w, g_1, g_2, \alpha$
d_F^k	$d+1$	-1	$d+2$	-2	d	0	1	-2	-1	y	$4-d$	0
d_F^ω	-1	1	-2	2	$1/2$	$-1/2$	0	1	1	0	0	0
d_F	$d-1$	1	$d-2$	2	$d+1$	-1	1	0	1	y	$4-d$	0

- (1) In any dynamical model of the type (3.1) all the 1-irreducible functions without the response fields v'_i or ϕ' necessarily contain closed circuits of retarded propagators. Therefore, such functions vanish identically, i.e., they do not require counterterms.
- (2) The field ϕ enters the vertex $\phi'(v_i\partial_i)\phi$ only in the form of a spatial derivative, which reduces the real index of divergence:

$$\delta'_\Gamma = \delta_\Gamma - N_\phi. \quad (3.10)$$

In particular, this means that the field ϕ enters the counterterms only in the form of the derivative $\partial_i\phi$. In fact, not all counterterms allowed by dimensional analysis are present. For example, for the 1-irreducible function $\langle\phi'\phi\rangle$ one obtains $\delta_\Gamma = 2$, $\delta'_\Gamma = 1$, thus, the only possible counterterm is $\phi'\partial^2\phi$, while the structure $\phi'\partial_t\phi$ is forbidden.

- (3) Since the random noise (2.7) is white in-time, the model (3.1) is Galilean invariant. Hence, the contributions of the counterterms have to respect this invariance. In particular, the covariant derivative (2.2) must enter the counterterms as a whole. This imposes some restrictions on possible counterterms: the counterterm required for the 1-irreducible function $\langle\phi'v_i\phi\rangle$ with $\delta_\Gamma = 1$, $\delta'_\Gamma = 0$, necessarily attains the form $\phi'(v_i\partial_i)\phi$ and can appear only in the combination $\phi'\nabla_t\phi$ with the counterterm $\phi'\partial_t\phi$ discussed above. Hence, it is forbidden.
- (4) An additional observation which reduces possible types of counterterms is the generalized Galilean invariance with the time-dependent vector transformation velocity parameter $\mathbf{w}(t)$:

$$\begin{aligned} \mathbf{v}_w(x) &= \mathbf{v}(x_w) - \mathbf{w}(t), & x &= (t, \mathbf{x}), \\ \Psi_w(x) &= \Psi(x_w); & x_w &= (t, \mathbf{x} + \mathbf{u}(t)); \\ \mathbf{u}(t) &= \int_{-\infty}^t \mathbf{w}(t') dt', \end{aligned} \quad (3.11)$$

where Ψ stands for any of the three remaining fields – v'_i, ϕ', ϕ . The crucial idea is that despite the fact that the action functional is not invariant with respect to such a transformation, it transforms in the identical way as the generating functional of the 1-irreducible Green functions:

$$\begin{aligned} \mathcal{S}_w(\Psi_w) &= \mathcal{S}_w(\Psi) + v'_i\partial_t w_i, \\ \Gamma(\Psi_w) &= \Gamma(\Psi) + v'_i\partial_t w_i. \end{aligned} \quad (3.12)$$

Since the latter formula can be rewritten in the form

$$\Gamma(\Phi) = \mathcal{S}(\Phi) + \tilde{\Gamma}(\Phi), \quad (3.13)$$

where Φ is the set of all the fields, $\Phi = \{v_i, v'_i, \phi, \phi'\}$, $\mathcal{S}(\Phi)$ is the given action functional, and $\tilde{\Gamma}(\Phi)$ is the sum of all the 1-irreducible loop diagrams that contain all the UV divergences. The expressions (3.12) mean that the counterterms appear invariant under the generalized Galilean transformation (3.11).

The above considerations exclude the counterterm $v'_i\nabla_t v_i$, invariant with respect to the conventional Galilean transformation with a constant vector \mathbf{w} , but not invariant with respect to (3.11). In particular, the only possible counterterm for 1-irreducible function $\langle v'_i v_j \rangle$ with $\delta_\Gamma = 2$ is $v'_i\partial^2 v_i$, and that the 1-irreducible function $\langle v'_i v_j v_k \rangle$ with $\delta_\Gamma = 1$ does not diverge. More detailed discussions of the application of the generalized Galilean transformation can be found in [8, 9, 14, 66, 67].

- (5) From the expressions (3.4) for propagators it follows that propagators containing the field ϕ , namely, $\langle v'_i\phi\rangle_0$, $\langle v_i\phi\rangle_0$, and $\langle\phi\phi\rangle_0$, contain the factors c_0^2 or c_0^4 . Since $d_c^k \neq 0$ and $d_c^\omega \neq 0$, parameter c_0 shows up as an external numerical factor in any diagram involving these propagators, and its real index of divergence reduces by the corresponding number of unities. In particular, any diagram of the 1-irreducible function with $N_{\phi'} > N_\phi$ must contain the factor $c_0^{2(N_{\phi'} - N_\phi)}$. It then follows that the counterterm to the 1-irreducible function $\langle\phi'v_j\rangle$ with $\delta_\Gamma = 3$ inevitably reduces to $c_0^2\phi'(\partial_j v_j)$, while the structures $\phi'\partial^2(\partial_j v_j)$, etc. are forbidden. Another consequence is UV finiteness of the 1-irreducible function $\langle\phi'v_i v_j\rangle$ with $\delta_\Gamma = 2$. Each diagram of this function contains the factor c_0^2 , which forbids the counterterms of the form $\phi'(\partial_i v_i)(\partial_j v_j)$, etc., while the remaining structure $c_0^2\phi'v^2$ is forbidden by the Galilean symmetry.
- (6) A crucial observation refers to the function $\langle v'_i v'_j \rangle$: the corresponding index of divergence reads $\delta_\Gamma = -d + 4$, therefore, it becomes UV divergent in $d = 2, 3$, and 4 and requires a presence of specific counterterms. For the physical case $d = 3$ ($\delta_\Gamma = 1$) it is impossible to construct a scalar counterterm containing two vector fields and one derivative¹, so the

¹ For the same reason the diagram $\langle v'_i v'_j v_k \rangle$ with $\delta_\Gamma = 3 - d$ does not diverge at $d = 3$.

only possible way is to include the UV cutoff Λ in the counterterm. Such counterterms do not involve poles in y (or $\varepsilon = 4 - d$, see later) and, therefore, they are lost if the calculations are performed using the formal rules of dimensional regularization and do not affect critical behavior. The situation is similar to the well-known ϕ^4 model, in which such counterterms leads to the shift of the parameter $\tau = T - T_c$, the deviation of the temperature from its critical value, which in theory of critical phenomena is an analogue of the mass term: $\tau_0 \rightarrow \tau_0 + g_0\Lambda^2$. The difference is that in our model there is no local term in (2.8), so this term should appear, with its own constant; see expression (3.3). But if $d < 4$ the new constant g_{20} is not dimensionless and, therefore, does not give rise to the additional beta function in the RG equations². This is why one can use the dimensional regularization in the analysis of the fixed points and in the calculation of critical exponents.

This means that in special space dimension $d = 3$ the renormalization group analysis is simplified and does not catch features associated with this divergence, and the results of [38, 55] should be treated as preliminary. A more fruitful approach is to study our model at $d = 2$ or $d = 4$, which may allow us to find new scaling regimes that can be applied to the physical value $d = 3$.

In this work we analyze the model (3.1) in the vicinity of the spatial dimension 4, which requires to take into account only one additional divergent function $\langle v'_i v'_j \rangle$. For this reason we have modified the kernel function $\tilde{D}_{ik}(\mathbf{k})$ [see (2.8) and (3.3)] and introduced the second coupling constant g_{20} and $\varepsilon = 4 - d$, which together with y plays the role of an expansion parameter. To explore this model at $d = 2$ one should consider four new divergent functions, namely, $\langle v'_i v'_j \rangle$ with $\delta_\Gamma = 2$, the functions

$\langle v'_i v'_j v'_k \rangle$ and $\langle v'_i v'_j v'_k \rangle$ with $\delta_\Gamma = 1$, and the function $\langle v'_i v'_j v'_k v'_l \rangle$ with $\delta_\Gamma = 0$, so it is a much more complicated task and a possible problem for the future studies [62].

Using all these considerations one can show that all the UV divergences in the model (3.1) near $d = 4$ can be removed by the counterterms of the form

$$\begin{aligned} v'_i \partial^2 v_i, & \quad v'_i \partial_i \partial_j v_j, & \quad v'_i \partial_i \phi, \\ c_0^2 \phi' \partial_i v_i, & \quad \phi' \partial^2 \phi, & \quad v'_i v'_i, \end{aligned} \quad (3.14)$$

which are already included in the extended action functional (3.1) with $v_0 > 0$. Now the poles can be eliminated by multiplicative renormalization of the parameters $g_{10}, g_{20}, \nu_0, u_0, v_0, c_0$ and the fields ϕ and ϕ' :

$$\begin{aligned} g_{10} &= g_1 \mu^y Z_{g_1}, & u_0 &= u Z_u, & \nu_0 &= \nu Z_\nu, \\ g_{20} &= g_2 \mu^\varepsilon Z_{g_2}, & v_0 &= v Z_v, & c_0 &= c Z_c. \end{aligned} \quad (3.15)$$

Here, μ is the scale-setting parameter (additional free parameter of the renormalized theory) in the MS scheme, the parameters g_1, g_2, ν, u, v , and c are renormalized analogs of the bare parameters (without subscript “0”), $Z_i, i \in \{g_1, g_2, u, v, \nu, c\}$, are the renormalization constants, which depend only on the completely dimensionless parameters $g_1, g_2, u, v, \alpha, d, y$ and ε . The fields ϕ and ϕ' are renormalized in the following way:

$$\phi \rightarrow Z_\phi \phi, \quad \phi' \rightarrow Z_{\phi'} \phi'. \quad (3.16)$$

The non-local part of the function D_{ik} does not require the renormalization, so it can be expressed in renormalized parameters using the relation $g_{10} \nu_0^3 = g_1 \nu^3 \mu^y$, see (3.18) below. The parameters m and α from the correlation function (2.7) are not renormalized: $Z_m = Z_\alpha = 1$. Due to the absence of renormalization of the term $v'_i \nabla_t v_i$ no renormalization of the fields v_i and v'_i is needed: $Z_v = Z_{v'} = 1$.

Hence, the renormalized action functional has the form

$$\begin{aligned} \mathcal{S}_v^R(\Phi) &= \frac{1}{2} v'_i D_{ij}^R v'_j + v'_i \left[-\nabla_t v_i + Z_1 \nu (\delta_{ij} \partial^2 - \partial_i \partial_j) v_j + Z_2 u \nu \partial_i \partial_j v_j - Z_4 \partial_i \phi \right] + \\ &+ \phi' \left[-\nabla_t \phi + Z_3 \nu \partial^2 \phi - Z_5 c^2 (\partial_i v_i) \right], \end{aligned} \quad (3.17)$$

where

$$D_{ij}^R = g_1 \mu^y \nu^3 p^{4-d-y} \left\{ P_{ij}(\mathbf{p}) + \alpha Q_{ij}(\mathbf{p}) \right\} + Z_6 g_2 \mu^\varepsilon \nu^3 \delta_{ij}. \quad (3.18)$$

In comparison to the case $d = 3$, there additional renormalization constant is needed, namely Z_6 .

² Detailed discussion of the similar situation in the RG analysis of the helical magnetohydrodynamic (MHD) turbulence can be found in the monographs [9], Secs. 6.16 and 6.17, and [14], Sec. 3.9.

IV. RENORMALIZATION OF THE MODEL

A. Perturbation expansion for the 1-irreducible Green functions

Let us consider the generating functional $\Gamma(\Phi)$ of the 1-irreducible Green functions. According to Eq. (3.13), $\Gamma(\Phi)$ can be written using the Legendre transform in the following form

$$\Gamma(\Phi) = \mathcal{S}_v(\Phi) + \tilde{\Gamma}(\Phi), \quad (4.1)$$

where for the functional arguments we have used the same symbols $\Phi = \{v_i, v'_j, \phi, \phi'\}$ as for the corresponding random fields. Here, $\mathcal{S}_v(\Phi)$ is the action functional (3.1)

and $\tilde{\Gamma}(\Phi)$ is the sum of all the 1-irreducible diagrams with loops. Hence, in the one-loop approximation, the expressions for the 1-irreducible Green functions that require UV renormalization take the form

$$\Gamma_{v'v} = i\omega - (\delta_{ij}p^2 - p_i p_j)Z_1\nu - p_i p_j Z_2 u\nu + \text{---}\overbrace{\text{---}}^{\text{---}}\text{---}, \quad (4.2)$$

$$\Gamma_{\phi\phi'} = i\omega - p^2 Z_3 v\nu + \text{---}\overbrace{\text{---}}^{\text{---}}\text{---}, \quad (4.3)$$

$$\Gamma_{v'\phi} = -iZ_4 p_i + \text{---}\overbrace{\text{---}}^{\text{---}}\text{---}, \quad (4.4)$$

$$\Gamma_{\phi'v} = -iZ_5 p_j c^2 + \text{---}\overbrace{\text{---}}^{\text{---}}\text{---} + \text{---}\overbrace{\text{---}}^{\text{---}}\text{---} + \text{---}\overbrace{\text{---}}^{\text{---}}\text{---}, \quad (4.5)$$

$$\Gamma_{v'v'} = g_1 \mu^y \nu^3 p^{4-d-y} \left\{ P_{ij}(\mathbf{p}) + \alpha Q_{ij}(\mathbf{p}) \right\} + Z_6 g_2 \mu^\varepsilon \nu^3 \delta_{ij} + \frac{1}{2} \text{---}\overbrace{\text{---}}^{\text{---}}\text{---}, \quad (4.6)$$

where \mathbf{p} stands for the corresponding external momentum. The factor 1/2 in front of the diagram in (4.6) is the symmetry coefficient of the graph; for all the other graphs the symmetry coefficients are equal to 1.

From a direct comparison of the relations between renormalized parameters it is straightforward to show that the renormalization constants in (3.15) and (4.2) – (4.6) are related as follows

$$\begin{aligned} Z_\nu &= Z_1, & Z_{g_1} &= Z_1^{-3}, & Z_c &= (Z_4 Z_5)^{1/2}, \\ Z_\phi &= Z_4, & Z_{\phi'} &= Z_4^{-1}, & Z_v &= Z_3 Z_1^{-1}, \\ Z_u &= Z_2 Z_1^{-1}, & Z_{g_2} &= Z_6 Z_1^{-3}. \end{aligned} \quad (4.7)$$

The renormalization constants are derived from the requirement that the Green functions of the renormalized model (3.17), when expressed in renormalized variables, be UV finite.

B. Renormalization constants

All diagram calculations are performed using dimensional regularization and the MS scheme, and can be found in Appendix A. All the diagrams are calculated in the arbitrary space dimension d , and only the poles in y and $\varepsilon = 4 - d$ are presented in the results.

The renormalization constants of the fields ϕ and ϕ' and the physical parameters of the system calculated from the diagrams and expressions (4.2) – (4.6) and (4.7) are:

$$\begin{aligned} Z_\nu &= 1 + A \left(\frac{g_1}{y} + \frac{g_2}{\varepsilon} \right) + B \left(\alpha \frac{g_1}{y} + \frac{g_2}{\varepsilon} \right); \\ Z_u &= 1 + (C - A) \left(\frac{g_1}{y} + \frac{g_2}{\varepsilon} \right) - B \left(\alpha \frac{g_1}{y} + \frac{g_2}{\varepsilon} \right); \end{aligned}$$

$$\begin{aligned} Z_v &= 1 - (A + D) \left(\frac{g_1}{y} + \frac{g_2}{\varepsilon} \right) \\ &\quad - (B + E) \left(\alpha \frac{g_1}{y} + \frac{g_2}{\varepsilon} \right); \\ Z_c &= 1 + \frac{1}{2} F \left(\frac{g_1}{y} + \frac{g_2}{\varepsilon} \right); \\ Z_\phi &= 1 + F \left(\frac{g_1}{y} + \frac{g_2}{\varepsilon} \right); \\ Z_{\phi'} &= 1 - F \left(\frac{g_1}{y} + \frac{g_2}{\varepsilon} \right); \\ Z_{g_1} &= 1 - 3A \left(\frac{g_1}{y} + \frac{g_2}{\varepsilon} \right) - 3B \left(\alpha \frac{g_1}{y} + \frac{g_2}{\varepsilon} \right); \\ Z_{g_2} &= 1 - 3A \left(\frac{g_1}{y} + \frac{g_2}{\varepsilon} \right) - 3B \left(\alpha \frac{g_1}{y} + \frac{g_2}{\varepsilon} \right) \\ &\quad - G \left[\alpha \frac{g_1^2}{g_2(2y - \varepsilon)} + (1 + \alpha) \frac{g_1}{y} + \frac{g_2}{\varepsilon} \right], \end{aligned} \quad (4.8)$$

where A, \dots, F are the coefficients from the renormalization constants $Z_1 - Z_6$ (see Appendix A):

$$\begin{aligned} A &= -\frac{d(d-1)u^2 + 2u(d^2 + d - 4) + d(d+3)}{4d(d+2)(u+1)^2}; \\ B &= -\frac{u-1}{2du(1+u)^2}; \\ C &= -(d-1) \frac{u^2(d-1) + u(d+4) + 1}{2d(d+2)u(u+1)^2}; \\ D &= \frac{d-1}{2dv(v+1)}; \\ E &= \frac{u-v}{2dvv(u+v)^2}; \\ F &= \frac{d-1}{2d(u+1)(v+1)}; \end{aligned}$$

$$G = \frac{d-1}{2du(u+1)}. \quad (4.9)$$

The expressions (4.8) contain all renormalization constants needed to renormalize our model near $d = 4$.

C. RG equations and functions

The relation between the initial and renormalized action functionals $\mathcal{S}(\Phi, e_0) = \mathcal{S}^R(Z_\Phi \Phi, e, \mu)$ (where e_0 is the complete set of bare parameters and e is the set of their renormalized counterparts) yields the fundamental RG differential equation:

$$\left\{ \mathcal{D}_{RG} + N_\phi \gamma_\phi + N_{\phi'} \gamma_{\phi'} \right\} G^R(e, \mu, \dots) = 0, \quad (4.10)$$

where $G = \langle \Phi \dots \Phi \rangle$ is a correlation function of the fields Φ ; N_ϕ and $N_{\phi'}$ are the counts of normalization-requiring fields ϕ and ϕ' , respectively, which are the inputs to G ; the ellipsis in expression (4.10) stands for the other arguments of G (spatial and time variables, etc.). \mathcal{D}_{RG} is the operation $\tilde{\mathcal{D}}_\mu$ expressed in the renormalized

variables and $\tilde{\mathcal{D}}_\mu$ is the differential operation $\mu \partial_\mu$ for fixed e_0 . For the present model it takes the form

$$\mathcal{D}_{RG} = \mathcal{D}_\mu + \beta_{g_1} \partial_{g_1} + \beta_{g_2} \partial_{g_2} + \beta_u \partial_u + \beta_v \partial_v - \gamma_\nu \mathcal{D}_\nu - \gamma_c \mathcal{D}_c. \quad (4.11)$$

Here, we have denoted $\mathcal{D}_x \equiv x \partial_x$ for any variable x . The anomalous dimension γ_F of some quantity F (a field or a parameter) is defined as

$$\gamma_F = Z_F^{-1} \tilde{\mathcal{D}}_\mu Z_F = \tilde{\mathcal{D}}_\mu \ln Z_F, \quad (4.12)$$

and the β functions for the four dimensionless coupling constants g_1 , g_2 , u and v , which express the flows of parameters under the RG transformation, are $\beta_g = \tilde{\mathcal{D}}_\mu g$. Together with (3.15) this yields

$$\begin{aligned} \beta_{g_1} &= g_1(-y - \gamma_{g_1}), & \beta_{g_2} &= g_2(-\varepsilon - \gamma_{g_2}), \\ \beta_u &= -u\gamma_u, & \beta_v &= -v\gamma_v. \end{aligned} \quad (4.13)$$

From the definitions and explicit expressions (4.8), (4.9) one finds in the one-loop approximation (i.e., with corrections of orders g_1^2 , g_2^2 , $g_1 g_2$ and higher) in $d = 4$:

$$\gamma_\nu = g_1 \frac{3u^2 + 8u + 7}{24(u+1)^2} + \alpha g_1 \frac{u-1}{8u(u+1)^2} + g_2 \frac{3u^3 + 8u^2 + 10u - 3}{24u(u+1)^2}; \quad (4.14)$$

$$\gamma_u = -\frac{u-1}{48u(u+1)^2} \left[g_1(6u^2 + 13u + 3) + 6\alpha g_1 + g_2(6u^2 + 13u + 9) \right]; \quad (4.15)$$

$$\begin{aligned} \gamma_v &= \frac{g_1}{24} \left[-\frac{3u^2 + 8u + 7}{(u+1)^2} + \frac{9}{v(v+1)} \right] - \alpha g_1 \frac{v-1}{8u(u+1)^2 v(u+v)^2} \left[u^3 + 2u^2(v+1) - v(v+1) + u(v^2 - v + 1) \right] \\ &+ \frac{g_2}{24} \left[-\frac{3(u-1)}{u(u+1)^2} - \frac{3u^2 + 8u + 7}{(u+1)^2} + \frac{3(u-v)}{uv(u+v)^2} + \frac{9}{v(v+1)} \right]; \end{aligned} \quad (4.16)$$

$$\gamma_c = -\frac{3}{16(u+1)(v+1)}(g_1 + g_2); \quad (4.17)$$

$$\gamma_\phi = -\frac{3}{8(u+1)(v+1)}(g_1 + g_2); \quad (4.18)$$

$$\gamma_{\phi'} = \frac{3}{8(u+1)(v+1)}(g_1 + g_2); \quad (4.19)$$

$$\gamma_{g_1} = -g_1 \frac{3u^2 + 8u + 7}{8(u+1)^2} - \alpha g_1 \frac{3(u-1)}{8u(u+1)^2} - g_2 \frac{3u^3 + 8u^2 + 10u - 3}{8u(u+1)^2}; \quad (4.20)$$

$$\gamma_{g_2} = \frac{1}{8u(u+1)^2} \left[-g_1(3u^3 + 8u^2 + 4u - 3) - g_2(3u^3 + 8u^2 + 7u - 6) + 3 \frac{\alpha g_1}{g_2} [(u+1)g_1 + 2g_2] \right]. \quad (4.21)$$

This means that from the expressions (4.13) and (4.14) – (4.21) all the functions entering the differential operator (4.11) are known, and, therefore, now we may consider how this differential operator acts on different Green functions. We do not include the dimensionless parameter α into the list of coupling constants, because it is not renormalized ($Z_\alpha = 1$) and the corresponding func-

tion β_α vanishes identically. Thus, the RG equations do not impose restrictions on the value of α , and α remains a free parameter of the model.

V. RENORMALIZATION GROUP AND CRITICAL SCALING

A. RG functions and IR attractive fixed points

From the analysis of the RG equation (4.10) it follows that the large scale behavior with respect to spatial and time scales is governed by the IR attractive (“stable”) fixed points $g^* \equiv \{g_1^*, g_2^*, u^*, v^*\}$, whose coordinates are found from the conditions [9–11]:

$$\beta_{g_1}(g^*) = \beta_{g_2}(g^*) = \beta_u(g^*) = \beta_v(g^*) = 0. \quad (5.1)$$

Consider a set of invariant couplings $\bar{g}_i = \bar{g}_i(s, g)$ with the initial data $\bar{g}_i|_{s=1} = g_i$. Here, $s = k/\mu$ and IR asymptotic behavior (i.e., behavior at large distances) corresponds to the limit $s \rightarrow 0$. An evolution of invariant couplings is described by the set of flow equations

$$\mathcal{D}_s \bar{g}_i = \beta_i(\bar{g}_j), \quad (5.2)$$

whose solution as $s \rightarrow 0$ behaves approximately like

$$\bar{g}_i(s, g^*) \cong g^* + \text{const} \times s^{\omega_i}, \quad (5.3)$$

where $\{\omega_i\}$ is the set of eigenvalues of the matrix

$$\Omega_{ij} = \partial\beta_i/\partial g_j|_{g=g^*}. \quad (5.4)$$

The existence of IR attractive solutions of the RG equations leads to the existence of the scaling behavior of Green functions. From (5.3) it follows that the type of the fixed point is determined by the matrix (5.4): for the IR attractive fixed points the matrix Ω has to be positive definite.

In contrast to the three dimensional case, where the analysis of the expressions like (4.13) and (4.14) – (4.21) has shown that in the physical range of parameters $g_1, u, v, \alpha > 0$ there exist only two IR attractive fixed points, one trivial (Gaussian) fixed point and one non-trivial [38, 55], at $d = 4$ situation is more intriguing: a direct analysis of the system of equations (5.1) reveals the existence of three IR attractive fixed points: a trivial free fixed point (FPI) and two non-trivial fixed points (FPII and FPIII).

The point FPI, for which all interactions are irrelevant and no scaling and universality is expected, has the coordinates

$$g_1^* = 0, \quad g_2^* = 0, \quad (5.5)$$

whereas the coordinates for couplings u^* and v^* are arbitrary. The corresponding eigenvalues of the matrix Ω_{ij} are

$$\lambda_1 = 0, \quad \lambda_2 = 0, \quad \lambda_3 = -\varepsilon, \quad \lambda_4 = -y. \quad (5.6)$$

Though trivial, FPI is necessary for the correct use of the perturbative renormalization group. From (5.6) it follows that FPI is IR attractive for negative values of y

and ε . Expressions (5.5) and (5.6) imply that in the four-dimensional space of coupling constants $\{g_1, g_2, u, v\}$ this fixed point is a “point” only in two dimensions $\{g_1, g_2\}$, and in the four-dimensional space of all couplings it is a two-dimensional plane. Zero eigenvalues λ_1 and λ_2 correspond to zero velocity along this plane, perpendicular to the plane (g_1, g_2) .

For the second fixed point, FPII, $g_1^* = 0$ while $g_2^* \neq 0$. Therefore, this scaling regime is called “local” [see (3.3)]. Its coordinates are

$$g_1^* = 0, \quad g_2^* = \frac{8\varepsilon}{3}, \quad u^* = 1, \quad v^* = 1. \quad (5.7)$$

The eigenvalues of the matrix Ω_{ij} are

$$\lambda_1 = \frac{7\varepsilon}{18}, \quad \lambda_2 = \frac{5\varepsilon}{6}, \quad \lambda_3 = \varepsilon, \quad \lambda_4 = \frac{3\varepsilon - 2y}{2}. \quad (5.8)$$

Thus, FPII is IR attractive in the region satisfying the inequalities $\varepsilon > 0$ and $y < 3\varepsilon/2$ and it is a node attractor, see discussion below.

For the last fixed point, FPIII, both the non-local and local parts of the random force are relevant:

$$g_1^* = \frac{16y(2y - 3\varepsilon)}{9[y(\alpha + 2) - 3\varepsilon]}, \quad g_2^* = \frac{16\alpha y^2}{9[y(\alpha + 2) - 3\varepsilon]}, \\ u^* = 1, \quad v^* = 1. \quad (5.9)$$

The corresponding eigenvalues of the matrix Ω_{ij} are

$$\lambda_1 = \frac{y[2y(10\alpha + 11) - 3\varepsilon(3\alpha + 11)]}{54[y(\alpha + 2) - 3\varepsilon]}, \\ \lambda_2 = \frac{y[2y(2\alpha + 3) - \varepsilon(\alpha + 9)]}{6[y(\alpha + 2) - 3\varepsilon]}, \\ \lambda_{3,4} = \frac{A \pm \sqrt{B}}{C}, \quad (5.10)$$

where the constants A , B , and C are given by

$$A = -27\varepsilon^3 + 9(\alpha + 9)\varepsilon^2 y - 9(3\alpha + 8)\varepsilon y^2 \\ + 2y^3(\alpha^2 + 7\alpha + 10); \\ B = [-3\varepsilon + (\alpha + 2)y]^2 [81\varepsilon^4 - 54\varepsilon^3 y - 9(20\alpha + 3)\varepsilon^2 y^2 \\ + 12(3\alpha^2 + 17\alpha + 1)\varepsilon y^3 - 4(5\alpha^2 + 14\alpha - 1)y^4]; \\ C = 6[-3\varepsilon + (\alpha + 2)y]^2. \quad (5.11)$$

Taking into account that in the physical range the couplings g_1 and g_2 must be positive, it follows from the explicit form of the eigenvalues $\lambda_1 \dots \lambda_4$ that the point FPIII is IR attractive when $y > 0$ and $y > 3\varepsilon/2$.

Furthermore, from the explicit form of the β functions β_u and β_v it readily follows that the 4×4 matrix Ω_{ij} decomposes to three blocks, the first two are 1×1 and the third is 2×2 . Two 1×1 blocks are determined by the eigenvalues $\lambda_1 = \partial\beta_u/\partial u|_{g=g^*}$ and $\lambda_2 = \partial\beta_v/\partial v|_{g=g^*}$, see (5.10). The remaining block, which needs to be diagonalized, is a 2×2 matrix, denoted $\tilde{\Omega}_{ij}$. This decomposition opens another opportunity to analyze whether

FPIII is IR attractive: the matrix $\tilde{\Omega}_{ij}$ is positive definite if and only if both $\text{Tr} \tilde{\Omega}_{ij} > 0$ and $\text{Det} \tilde{\Omega}_{ij} > 0$. In our case

$$\begin{aligned} \text{Tr} \tilde{\Omega}_{ij} &= \frac{9\varepsilon^2 - 12\varepsilon y + 2(\alpha + 5)y^2}{3[(\alpha + 2)y - 3\varepsilon]}; \\ \text{Det} \tilde{\Omega}_{ij} &= y \left(\frac{2}{3}y - \varepsilon \right). \end{aligned} \quad (5.12)$$

From (5.12) it follows that the matrix $\tilde{\Omega}_{ij}$ is positive in the region $y > 0$ and $y > 3\varepsilon/2$. This approach is simpler than direct analysis of the expressions (5.10) – (5.11), but does not distinguish a simple node attractor from a more complicated spiral attractor. The latter is a consequence of a non-zero imaginary part in the eigenvalues of the matrix Ω_{ij} .

The ability to determine whether an IR attractive fixed point corresponds to a node or a spiral attractor is an advantage of the double y and ε expansion near $d = 4$. Indeed, in the case of a simplified analysis near $d = 3$ [38, 55], Ω_{ij} is a 3×3 matrix and its eigenvalues³ are

$$\lambda_1 = y; \quad \lambda_2 = \frac{\alpha + 6}{12}y; \quad \lambda_3 = \frac{5\alpha + 12}{96}y. \quad (5.13)$$

From expressions (5.13) it follows that all the eigenvalues ($\lambda_1, \lambda_2, \lambda_3$) are real. Therefore, the fixed point is a node attractor. Nevertheless, this point may be a spiral attractor at large values of y , but we are not able to investigate this question near $d = 3$.

However, we can perform this analysis near $d = 4$. The quantity B [see (5.11)] is a fourth order polynomial in the exponent y . From its analysis it follows that if $\alpha \leq \frac{1}{5}(-7 + 3\sqrt{6}) \approx 0.07$, which is a positive root of the equation $5\alpha^2 + 14\alpha - 1 = 0$, the expression B is strictly positive in the region $y > 0$, $y > 3\varepsilon/2$. That is, in this case FPIII is a node attractor for all permissible values of y and ε . If $\alpha > \frac{1}{5}(-7 + 3\sqrt{6})$, equation $B(y) = 0$ has one root $R(\alpha, \varepsilon)$, that is larger than $3\varepsilon/2$. Thus, if $3\varepsilon/2 < y < R(\alpha, \varepsilon)$, FPIII is a node attractor; whereas if $y > R(\alpha, \varepsilon)$, the eigenvalues λ_3 and λ_4 contain non-zero imaginary parts and FPIII is a spiral attractor. An abrupt change from a node to a spiral attractor in the region $y > R(\alpha, \varepsilon)$ near the point $\alpha = \frac{1}{5}(-7 + 3\sqrt{6})$ (especially at $\varepsilon < 0$) looks intriguing, but may be an artifact of the one-loop approximation we used.

³ Note, that in previous study [38] there are misprints in the expressions (2.25) and (2.28) for the constant Z_3 and function $A(d)$, which enter into expressions for β functions β_g, β_u , and β_v . The correct expressions read

$$Z_3 = 1 - \frac{\hat{g}}{y} \frac{d-1}{2dv(v+1)} - \frac{\alpha\hat{g}}{y} \frac{u-v}{2dvv(u+v)^2}$$

and

$$A = \frac{-d(d-1)u^2 - 2(d^2 + d - 4)u - d(d+3)}{4d(d+2)(1+u)^2} + \frac{\alpha(1-u)}{2du(1+u)^2}.$$

The explicit expression for $R(\alpha, \varepsilon)$, being a solution of the fourth degree polynomial equation, is rather cumbersome and, therefore, is omitted here. We have computed that

$$\lim_{\alpha \rightarrow \infty} R(\alpha, \varepsilon) = \frac{9\varepsilon}{5}, \quad (5.14)$$

which is in agreement with (5.28), obtained as a result of the analysis performed directly at $\alpha = \infty$. This means that the crossover between node and spiral attractors takes place along the line $R(\alpha, \varepsilon)$, which is vertical at α near $\frac{1}{5}(-7 + 3\sqrt{6})$ and rotates clockwise toward the line $R(\infty, \varepsilon) = 9\varepsilon/5$ as $\alpha \rightarrow \infty$ (see Fig. 4).

At the real values of the parameters $y = 4$ and $\varepsilon = 1$ FPIII is a spiral attractor for $\alpha > \frac{5}{176}(-26 + 9\sqrt{15}) \approx 0.251$.

To complete the analysis of the fixed point structure, infinite fixed point values $u \rightarrow \infty$ and $v \rightarrow \infty$ have to be considered as well. Since u may be interpreted as longitudinal viscosity, from the physical point of view this case corresponds to the limit $c \rightarrow \infty$. Here, the velocity fields v_i and v'_i are purely transverse and the scalar fields ϕ and ϕ' are effectively decoupled from them; see the explicit expressions for propagators (3.4). By introducing a new variable $f = 1/u$ with its β function

$$\beta_f = \tilde{\mathcal{D}}_\mu f = -f^2 \beta_u, \quad (5.15)$$

one obtains the following set of β functions at $f = 0$:

$$\begin{aligned} \beta_{g_1} &= \frac{1}{8}g_1(3g_1 + 3g_2 - 8y); \\ \beta_{g_2} &= \frac{1}{8}g_2(3g_1 + 3g_2 - 8\varepsilon); \\ \beta_v &= \frac{1}{8}(g_1 + g_2) \frac{v^2 + v - 3}{v + 1}. \end{aligned} \quad (5.16)$$

From (5.15) and (5.16) it follows that there are two non-trivial fixed points for $f^* = 0$:

$$g_1^* = 0, \quad g_2^* = 8\varepsilon/3, \quad v^* = \frac{1}{2}(-1 + \sqrt{13}); \quad (5.17)$$

$$g_1^* = 8y/3, \quad g_2^* = 0, \quad v^* = \frac{1}{2}(-1 + \sqrt{13}). \quad (5.18)$$

However, two of the four eigenvalues have opposite signs at any values of y and ε , namely

$$\lambda_1 = -y/3, \quad \lambda_2 = \frac{2(13 + \sqrt{13})}{3(1 + \sqrt{13})^2}y \quad (5.19)$$

for the fixed point given by Eq. (5.17), whereas

$$\lambda_1 = -\varepsilon/3, \quad \lambda_2 = \varepsilon \quad (5.20)$$

for the fixed point given by Eq. (5.18).

Thus, both fixed point (5.17) and (5.18) are unstable (i.e., saddle points). This agrees with the observation that the leading-order correction in the Mach number

to the incompressible scaling regime destroys its stability [52–54].

In order to study the limit $v \rightarrow \infty$, let us create a new variable $t = 1/v$ with β function

$$\beta_t = \tilde{D}_\mu t = -t^2 \beta_v. \quad (5.21)$$

For $t = 0$ one obtains $\beta_t = 0$. Since β functions of the other coupling constants g_1 , g_2 , and u are independent of v , at $t = 0$ we recognize the formerly obtained fixed points II and III. Thus, to investigate the IR attraction of these two points, one should only check the derivative $\partial\beta_t/\partial t$ at the fixed point $\{g^*, t = 0\}$:

$$\begin{aligned} \lambda_t &= -\varepsilon/2 \quad \text{for FPII;} \\ \lambda_t &= -y/3 \quad \text{for FPIII.} \end{aligned} \quad (5.22)$$

Comparing (5.22) with (5.8) and (5.10), we find that in the limit $v \rightarrow \infty$ these two fixed points are saddle points as well.

In contrast to the direct analysis near three-dimensional case $d = 3$ (see [38]), where non-trivial IR attractive fixed point was valid for all $\alpha > 0$, had finite limit at $\alpha \rightarrow \infty$, but was unstable at $\alpha = \infty$ (i.e., in the case of a purely potential random force), under this analysis near $d = 4$ the situation is much better. Taking into account (3.3), to study this limit we define new coupling constant $g'_1 = g_1\alpha$, which is finite as $\alpha \rightarrow \infty$; g_2 herewith does not change, i.e., $g'_2 = g_2$. Hence, since $Z_\alpha = 1$, a new β function is

$$\beta_{g'_1} = \tilde{D}_\mu g'_1 = \alpha\beta_{g_1}, \quad (5.23)$$

and the full set of β functions is:

$$\begin{aligned} \beta_{g'_1} &= g'_1 \left[-y + \frac{g_2(3u^3 + 8u^2 + 10u - 3) + 3g'_1(u-1)}{8u(u+1)^2} \right]; \\ \beta_{g_2} &= g_2 \left[-\varepsilon + \frac{g_2(3u^3 + 8u^2 + 7u - 6) - 6g'_1}{8u(u+1)^2} \right]; \\ \beta_u &= \frac{u-1}{48(u+1)^2} [6g'_1 + g_2(6u^2 + 13u + 9)]; \\ \beta_v &= g'_1 \frac{v-1}{8u(u+1)^2(u+v)^2} \\ &\quad \times [u^3 + 2u^2(v+1) - v(v+1) + u(v^2 - v + 1)] \\ &\quad - g_2 \frac{v}{24} \left[\frac{3(1-u)}{u(u+1)^2} - \frac{7+8u+3u^2}{(u+1)^2} \right. \\ &\quad \left. + \frac{3(u-v)}{uv(u+v)^2} + \frac{9}{v(v+1)} \right]. \end{aligned} \quad (5.24)$$

The solution of the system (5.1) in this case allows three IR attractive fixed points: a trivial one

$$g'_1 = 0, \quad g_2 = 0, \quad (5.25)$$

with u^* and v^* undetermined, which is IR attractive when $y < 0$ and $\varepsilon < 0$; a local one

$$g'_1 = 0, \quad g_2 = \frac{8\varepsilon}{3}, \quad u^* = 1, \quad v^* = 1, \quad (5.26)$$

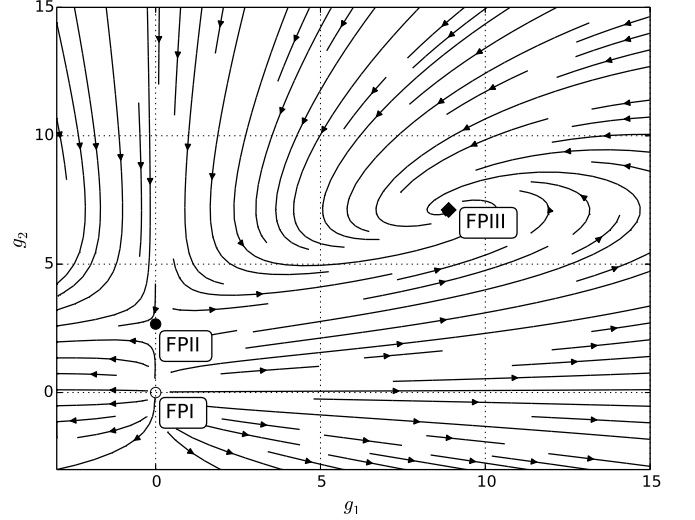


FIG. 3. RG flow diagram in the plane (g_1, g_2) at $y = 4$ and $\varepsilon = 1$; $\alpha = \infty$; $u = v = 1$. Three fixed points FPI, FPII, and FPIII are marked by an empty circle, a filled circle, and a filled rhombus, respectively.

which is IR attractive when $\varepsilon > 0$ and $y < 3\varepsilon/2$; and a non-local one

$$g'_1 = \frac{16}{9}(2y - 3\varepsilon), \quad g_2 = \frac{16y}{9}, \quad u^* = 1, \quad v^* = 1, \quad (5.27)$$

which is IR attractive when $y > 0$ and $y > 3\varepsilon/2$. The latter, being a non-local fixed point in the case of a purely potential random force, can be obtained from expressions (5.9) in the limit $\alpha \rightarrow \infty$, taking together with the substitution $g_1 = g'_1/\alpha$. Thus, in contrast to the simplified analysis near $d = 3$ [38, 55], the analysis near $d = 4$ provides a non-local fixed point (5.9), which has a finite limit as $\alpha \rightarrow \infty$, corresponding to a longitudinal random force.

The eigenvalues of the matrix Ω_{ij} in this case equal to

$$\begin{aligned} \lambda_1 &= \frac{1}{6}(-\varepsilon + 4y); & \lambda_2 &= \frac{1}{54}(-9\varepsilon + 20y); \\ \lambda_3 &= \frac{1}{3} \left[y - \sqrt{(9\varepsilon - 5y)y} \right]; & \lambda_4 &= \frac{1}{3} \left[y + \sqrt{(9\varepsilon - 5y)y} \right]. \end{aligned} \quad (5.28)$$

None of these eigenvalues contain an imaginary part if $y < 9\varepsilon/5$. Thus, a node attractor is realized if $3\varepsilon/2 < y < 9\varepsilon/5$ and a spiral attractor is realized if $y > 9\varepsilon/5$.

An RG flow diagram in the plane (g_1, g_2) for $u = v = 1$, $\alpha = \infty$, and real values of the parameters $y = 4$ and $\varepsilon = 1$ is shown in Fig. 3. The coordinates of three fixed points FPI, FPII, and FPIII are given by expressions (5.25) – (5.27). This diagram implies that at these values of y and ε FPI is IR repulsive point, FPII is a saddle point, and FPIII is a spiral attractor, in agreement with aforementioned analysis.

A general pattern of the stability of three fixed points in the plane (y, ε) is shown in Fig. 4. The lines $y < 0$,

$\varepsilon = 0$; $y = 0$, $\varepsilon < 0$; and $y = 3\varepsilon/2$, $\varepsilon > 0$ denote the boundaries of the domains, which have neither gaps between them nor overlaps. The crossover between two non-trivial fixed points takes place along the line $y = 3\varepsilon/2$, which is in accordance with [37]. The dotted line $y = 9\varepsilon/5$ corresponds to $\lim_{\alpha \rightarrow \infty} R(\alpha, \varepsilon)$ [see (5.14)] and indicates a boundary between areas in which the IR attractive point FPIII is a node ($3\varepsilon/2 < y < 9\varepsilon/5$) or a spiral ($y > 9\varepsilon/5$) attractor at $\alpha = \infty$.

The presence of the different IR attractive fixed points in the model (3.1) implies that depending on the values y and ε the correlation functions of the model in the IR region exhibit various types of scaling behavior.

The point FPII [see (5.7)] is a fixed point of a self-contained renormalizable local field theory, in which quadratic form (3.2) reduces to a single integral:

$$v'_i D_{ik} v'_k = g_{20} v_0^3 \int dt \int d^d \mathbf{x} v^2(t, \mathbf{x}). \quad (5.29)$$

This regime corresponds to the “compressible” analog of model B in the pioneering paper [61]. The authors interpret that this model describes a macroscopic “shaking” of a fluid container (the idea suggested by P. C. Martin, see footnote 15 in [61]), which is problem of a special (clear, practical) interest. The unavoidable presence of a local term in FPIII [see (5.9)] means that the non-local stirring force (2.7), due to the renormalization and the intrinsic non-linearity of the problem, gives rise to the effective “shaking” effect.

For the incompressible case, a new scaling regime arises near the dimension $d = 2$, see [58]. This regime formally corresponds to a fluid in thermal equilibrium (model A in [61]). To avoid misunderstanding, it should be stressed that the true thermal noise does not come into play in turbulence dynamics, but the non-local noise gives rise, due to the non-linear nature of the whole problem, to effective thermal-like noise. The situation resembles “effective turbulent diffusion,” in which the behavior of a particle in a turbulent environment resembles ordinary diffusion, but with coefficients determined by the characteristics of the turbulent flow.

The corresponding critical dimensions $\Delta[F] \equiv \Delta_F$ for all basic fields and parameters can be computed as series in a set of parameters y and ε , where y and ε are assumed to be quantities of the same order, i.e., $0 < y/\varepsilon < \infty$. If, for the real values $y = 4$ and $\varepsilon = 1$, the local point FPII were IR attractive, the IR behavior of the full non-local model would be the same as for the local case described by the fixed point (5.7) with the dimensions given in (5.36). Our findings show that this is not the case, and the IR behavior is governed by the dimensions (5.37); see next subsection for details.

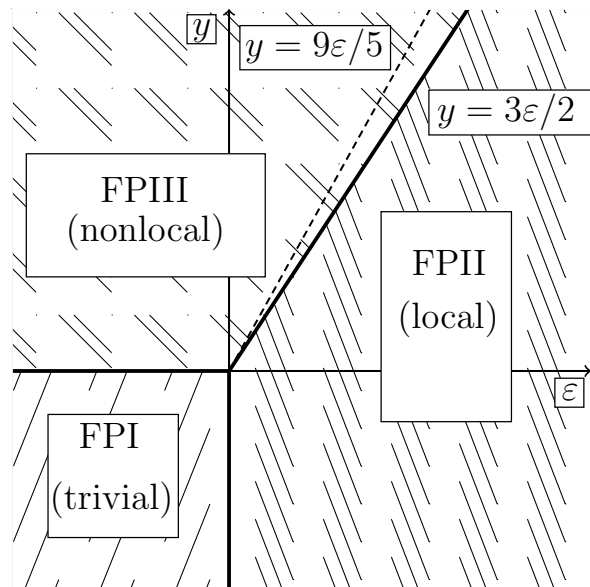


FIG. 4. Domains of IR stability of the fixed points for the model (3.1) in the plane (y, ε) .

B. IR attractive fixed points and critical dimensions

In the leading order the IR asymptotic behavior of the (renormalized) Green functions G^R satisfy the RG equation (4.10) with the substitution $g \rightarrow g_*$ for the full set of the couplings $\{g_1, g_2, u, v\}$, see [9, 11]. This yields

$$\left\{ \mathcal{D}_\mu - \gamma_\nu^* \mathcal{D}_\nu - \gamma_c^* \mathcal{D}_c + \sum_{\Phi} N_{\Phi} \gamma_{\Phi}^* \right\} G^R = 0. \quad (5.30)$$

Here, γ_F^* is the value of the anomalous dimension at the fixed point; the summation over all types of the fields Φ is implied. Equations of this type describe the scaling with dilatation of the variables whose derivatives enter the differential operator.

From (4.14) – (4.21) one obtains that in the one-loop approximation the expressions for the anomalous dimensions γ_F^* for the non-local point FPIII coincide with the case of $d = 3$:

$$\begin{aligned} \gamma_\nu^* &= y/3, & \gamma_\phi^* &= -\gamma_{\phi'}^* = -y/6 + \mathcal{O}(y^2), \\ \gamma_c^* &= -y/12 + \mathcal{O}(y^2). \end{aligned} \quad (5.31)$$

The expression for γ_ν^* is exact due to the relation between Z_ν and Z_{g_1} , see (4.7). For the local point FPII one obtains⁴

$$\begin{aligned} \gamma_\nu^* &= \varepsilon/2 + \mathcal{O}(\varepsilon^2), & \gamma_\phi^* &= -\gamma_{\phi'}^* = -\varepsilon/4 + \mathcal{O}(\varepsilon^2), \\ \gamma_c^* &= -\varepsilon/8 + \mathcal{O}(\varepsilon^2). \end{aligned} \quad (5.32)$$

⁴ There is a misprint in expression for γ_ν^* in published version.

The canonical scale invariance is expressed by two relations

$$\left\{ \sum_{\sigma} d_{\sigma}^k \mathcal{D}_{\sigma} - d_G^k \right\} G^R = 0, \quad \left\{ \sum_{\sigma} d_{\sigma}^{\omega} \mathcal{D}_{\sigma} - d_G^{\omega} \right\} G^R = 0, \quad (5.33)$$

where σ is the full set of all the arguments of G^R , d^k and d^{ω} are canonical dimensions. In order to derive the scaling with fixed ‘‘IR irrelevant’’ parameters μ and ν one has to combine Eqs. (5.30) and (5.33) such that the derivatives with respect to these parameters are eliminated; see [9, 14]. This yields an equation of critical IR scaling for the model

$$\left\{ -\mathcal{D}_{\mathbf{x}} + \Delta_t \mathcal{D}_t + \Delta_c \mathcal{D}_c + \Delta_m \mathcal{D}_m - \sum_{\Phi} N_{\Phi} \Delta_{\Phi} \right\} G^R = 0 \quad (5.34)$$

with the notation

$$\Delta_F = d_F^k + \Delta_{\omega} d_F^{\omega} + \gamma_F^*, \quad \Delta_{\omega} = -\Delta_t = 2 - \gamma_{\nu}^*. \quad (5.35)$$

Here, Δ_F is the critical dimension of the quantity F , while Δ_t and Δ_{ω} are the critical dimensions of the time and the frequency.

From Table I and Eqs. (5.31) and (5.32) we see that for the local point FPII critical dimensions take the form

$$\begin{aligned} \Delta_v &= 1 - \varepsilon/2, & \Delta_{v'} &= d - \Delta_v, \\ \Delta_{\omega} &= 2 - \varepsilon/2, & \Delta_m &= 1, \\ \Delta_{\phi} &= d - \Delta_{\phi'} = 2 - 5\varepsilon/4, & \Delta_c &= 1 - 5\varepsilon/8, \end{aligned} \quad (5.36)$$

whereas for the point FPIII they coincide with the case $d = 3$, namely,

$$\begin{aligned} \Delta_v &= 1 - y/3, & \Delta_{v'} &= d - \Delta_v, \\ \Delta_{\omega} &= 2 - y/3, & \Delta_m &= 1, \\ \Delta_{\phi} &= d - \Delta_{\phi'} = 2 - 5y/6, & \Delta_c &= 1 - 5y/12. \end{aligned} \quad (5.37)$$

Expressions (5.36) and (5.37) implies that depending on the values y and ε correlation functions can exhibit different types of scaling behavior in the IR region (local regime FPII or non-local regime FPIII) with different anomalous and critical dimensions.

VI. ADVECTION OF PASSIVE SCALAR FIELDS

The analysis of the passive advection bears a close resemblance to the case $d = 3$ (see [38]), so we will restrict ourselves to the main points.

A. Field theoretic formulation of the model

Consider a passive advection of a scalar density field $\theta(x) \equiv \theta(t, \mathbf{x})$ (e.g., density of a pollutant), which satisfies the stochastic differential equation

$$\partial_t \theta + \partial_i (v_i \theta) = \kappa_0 \partial^2 \theta + f_{\theta}. \quad (6.1)$$

Another related problem, which corresponds to the transformation $\partial_i (v_i \theta) \rightarrow (v_i \partial_i) \theta$ in the left hand side, has an interpretation of passive advection of a tracer field (e.g., temperature, concentration of the impurity particles, etc.); see [64]. As usual, $\partial_t \equiv \partial/\partial t$, $\partial_i \equiv \partial/\partial x_i$; κ_0 is the molecular diffusivity coefficient, $\partial^2 = \partial_i \partial_i$ is the Laplace operator, $v_i(x)$ is the velocity field, which obeys Eq. (2.1), and $f_{\theta} \equiv f_{\theta}(x)$ is a Gaussian noise with zero mean and given covariance

$$\langle f_{\theta}(x) f_{\theta}(x') \rangle = \delta(t - t') C(\mathbf{r}/\mathcal{L}_{\theta}), \quad \mathbf{r} = \mathbf{x} - \mathbf{x}'. \quad (6.2)$$

The function $C(\mathbf{r}/\mathcal{L}_{\theta})$ in Eq. (6.2) is finite at $(\mathbf{r}/\mathcal{L}_{\theta}) \rightarrow 0$ and rapidly decays when $(\mathbf{r}/\mathcal{L}_{\theta}) \rightarrow \infty$. Expression (6.2) brings about another large (integral) scale \mathcal{L}_{θ} , related to the noise variable f_{θ} , but henceforth we will not distinguish it from its analog $\mathcal{L} = m^{-1}$ in the correlation function of the stirring force (2.7). The noise is needed to maintain the steady state of the system, and in this respect it accounts for the effects of initial and/or boundary conditions.

In the absence of the noise, Eq. (6.1) acquires the form of a continuity equation (conservation law); θ being the density of a corresponding conserved quantity. If the function in (6.2) is chosen in such a way that its Fourier transform $C(\mathbf{k})$ vanishes at $\mathbf{k} = 0$, the fields θ or θ' remain to be conserved in statistical sense in the presence of the external stirring.

The advection of scalar fields in the case of Kraichnan’s rapid-change velocity ensemble were thoroughly studied [42–49]; the case of Gaussian velocity statistics with finite correlation time was studied in [50, 51].

If velocity v_i obeys the stochastic Navier-Stokes equation (2.1), the problem (6.1), (6.2) is tantamount to the field theoretic model of the full set of fields $\tilde{\Phi} \equiv \{\theta', \theta, v'_i, v_i, \phi', \phi\}$ and the action functional

$$\mathcal{S}(\tilde{\Phi}) = \mathcal{S}_{\theta}(\theta', \theta, v_i) + \mathcal{S}_v(v'_i, v_i, \phi', \phi). \quad (6.3)$$

The advection-diffusion component

$$\mathcal{S}_{\theta}(\theta', \theta, v_i) = \frac{1}{2} \theta' D_f \theta' + \theta' [-\partial_t \theta - \partial_i (v_i \theta) + \kappa_0 \partial^2 \theta] \quad (6.4)$$

in Eq. (6.3) is the De Dominicis-Janssen action for the stochastic problem (6.1), (6.2) at fixed v_i , while the second term is given by (3.1) and represents the velocity statistics; D_f is the correlation function (6.2), all the required integrations and summations over the vector indices are assumed.

In addition to (3.4), the diagrammatic technique in the full problem involves a new vertex $V_j^3 = -\theta' \partial_j (v_j \theta)$ and two new propagators

$$\begin{aligned} \langle \theta \theta' \rangle_0 &= \overline{\langle \theta' \theta \rangle_0} = \frac{1}{-i\omega + \kappa_0 k^2}, \\ \langle \theta \theta \rangle_0 &= \frac{C(\mathbf{k})}{\omega^2 + \kappa_0^2 k^4}. \end{aligned} \quad (6.5)$$



FIG. 5. Graphical representation of the bare propagators $\langle\theta'\theta\rangle_0$ and $\langle\theta\theta\rangle_0$.

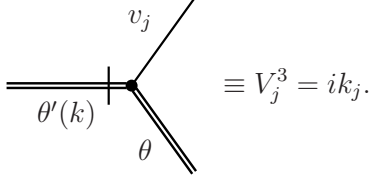


FIG. 6. Graphical representation of the interaction vertex V_j^3 .

From now a double solid line without a slash denotes the field θ , and a double solid line with a slash corresponds to the field θ' ; see Fig. 5. The vertex V_j^3 is depicted on Fig. 6 and in the momentum representation is given by

$$V_j^3(\mathbf{k}) = ik_j, \quad (6.6)$$

where \mathbf{k} is the momentum carried by the field θ' .

B. Renormalization of the model

Canonical dimensions of the new fields and parameters of the full model (6.3) can be found in Table I. The formal index of UV divergence (3.9) remains valid, but now the summation has to run over the full set of six fields $\tilde{\Phi} \equiv \{\theta', \theta, v'_i, v_i, \phi', \phi\}$. Rules (1) – (6) from Sec. IIIB have to be generalized and augmented:

- (7) All the 1-irreducible Green functions without any response fields $\tilde{\Phi}'$ vanish identically and require no counterterms.
- (8) Using the integration by parts the derivative at the vertex $-\theta'\partial_i(v_i\theta)$ can be moved onto the field θ' , therefore, Eq. (3.10) is modified:

$$\delta'_\Gamma = \delta_\Gamma - N_\phi - N_{\theta'}. \quad (6.7)$$

Since the field θ' can enter the counterterms only in the form of spatial derivatives, the counterterm $\theta'\partial_t\theta$ to the 1-irreducible Green function $\langle\theta'\theta\rangle$ with $\delta_\Gamma = 2$, $\delta'_\Gamma = 1$ is forbidden. Also this requires that the counterterms to the 1-irreducible function $\langle\theta'v_i\theta\rangle$ with $\delta_\Gamma = 1$, $\delta'_\Gamma = 0$ necessarily reduce to the form $\theta'\partial_i(v_i\theta)$. Galilean symmetry allows them to enter the counterterms only in the form of invariant combination $\theta'\nabla_t\theta$. Hence, they are also forbidden.

- (9) As a consequence of the linearity of the original stochastic equation (6.1) with respect to the field θ one obtains that for any 1-irreducible function the relation $N_{\theta'} - N_\theta = 2N_0$ is valid (here $N_0 \geq 0$ is the total number of bare propagators $\langle\theta\theta\rangle_0$ entering the diagram). This fact is very important for the

renormalizability of the model: without the restriction $N_\theta \leq N_{\theta'}$, the infinite number of superficially divergent 1-irreducible functions $\langle\theta'\theta\dots\theta\rangle$ would proliferate, and hence the lack of renormalizability would follow.

From these rules we finally conclude that superficial divergences can be present only in the 1-irreducible Green function $\langle\theta'\theta\rangle$ with the only counterterm $\theta'\partial^2\theta$. It is naturally reproduced as multiplicative renormalization of the diffusion coefficient, $\kappa_0 = \kappa Z_\kappa$. No renormalization of the fields θ' and θ is needed: $Z_{\theta'} = Z_\theta = 1$. Altogether, the renormalized analog of the action functional (6.3) takes the form

$$\mathcal{S}^R(\tilde{\Phi}) = \mathcal{S}_\theta^R(\theta', \theta, v_i) + \mathcal{S}_v^R(v'_i, v_i, \phi', \phi), \quad (6.8)$$

where \mathcal{S}_v^R is the action (3.17),

$$\mathcal{S}_\theta^R(\theta', \theta, v_i) = \frac{1}{2}\theta' D_f \theta' + \theta' [-\partial_t\theta - \partial_i(v_i\theta) + \kappa Z_\kappa \partial^2\theta]; \quad (6.9)$$

D_f here stands for the covariance of the stochastic force given by the Eq. (6.2).

C. Calculation of the diagram, fixed points and critical dimensions

The one-loop approximation for the 1-irreducible response function $\langle\theta'\theta\rangle$ can be formally written as

$$\Gamma_{\theta'\theta} = +i\omega - \kappa_0 p^2 + \text{diagram}, \quad (6.10)$$

where, as earlier in the expressions (4.2) – (4.6), \mathbf{p} stands for an external momentum entering the diagram; the single solid line denotes the bare propagator $\langle vv\rangle_0$ from (3.4), the double solid line with a slash denotes the bare propagator $\langle\theta'\theta\rangle_0$ from (6.5), the slashed end corresponds to the field θ' . The interaction vertex with three attached fields θ', θ and v contains the factor (6.6).

The renormalization constant Z_κ should be chosen as

$$Z_\kappa = 1 - \frac{1}{2dw} \left[\frac{d-1}{w+1} + \frac{\alpha(u-w)}{u(u+w)^2} \right] \frac{g_1}{y} - \frac{1}{2dw} \left[\frac{d-1}{w+1} + \frac{u-w}{u(u+w)^2} \right] \frac{g_2}{\varepsilon}, \quad (6.11)$$

where we introduced the new dimensionless coefficient $w_0 = \nu_0/\kappa_0$ with ν_0 from (2.1) and its renormalized analog w . The corresponding anomalous dimension is

$$\gamma_\kappa = \frac{1}{2dw} \left[\frac{d-1}{w+1} + \frac{\alpha(u-w)}{u(u+w)^2} \right] g_1 + \frac{1}{2dw} \left[\frac{d-1}{w+1} + \frac{u-w}{u(u+w)^2} \right] g_2, \quad (6.12)$$

with the possible corrections coming from higher orders terms; see Appendix B1 for details.

The function $\beta_w = \tilde{D}_\mu w$ for the new parameter w takes the form

$$\beta_w = -w\gamma_w = w(\gamma_\nu - \gamma_\kappa), \quad (6.13)$$

see Sec. IV C. Now the coordinates $\{g^*\}$ of the fixed points FPII and FPIII [see (5.7) and (5.9)] are substituted into the equation $\beta_w = 0$ at $d = 4$. We can rewrite the expression for $\gamma_\nu - \gamma_\kappa$ at $u = 1$:

$$\begin{aligned} \gamma_\nu - \gamma_\kappa|_{u=1} = & \frac{w-1}{16w(w+1)^2} [g_1(3w^2 + 9w + 2\alpha + 6) \\ & + g_2(3w^2 + 9w + 8)]. \end{aligned} \quad (6.14)$$

From Eq. (6.14) it is clear that the only positive solution for both FPII and FPIII is

$$w^* = 1. \quad (6.15)$$

The functions (4.13) do not depend on w . Therefore, a new eigenvalue of the matrix (5.4), corresponding to this parameter, coincides with the diagonal element $\partial\beta_w/\partial w$ at the point $\{g\} = \{g^*\}$:

$$\begin{aligned} \lambda_w = \frac{5\varepsilon}{6} > 0 \quad \text{for FPII;} \\ \lambda_w = \frac{2y}{3} + \frac{4\alpha y(y-\varepsilon)}{3[y(\alpha+2)-3\varepsilon]} > 0 \quad \text{for FPIII.} \end{aligned} \quad (6.16)$$

From the inequalities (6.16) it follows that the fixed points with the coordinates (5.7) and (5.9) and $w_* = 1$ are IR attractive in the full space of couplings $\{g_1, g_2, u, v, w\}$ and govern the IR asymptotic behavior of the full-scale model (6.3).

The critical dimensions of the passive fields θ and θ' are obtained from Table I and Eq. (5.35) for Δ_ω . For FPII they are

$$\Delta_\theta = -1 + \varepsilon/4, \quad \Delta_{\theta'} = d + 1 - \varepsilon/4; \quad (6.17)$$

for FPIII they are the same as in the case $d = 3$, namely,

$$\Delta_\theta = -1 + y/6, \quad \Delta_{\theta'} = d + 1 - y/6. \quad (6.18)$$

D. Renormalization and critical dimensions of composite operators

In the following, the central role is played by composite fields (“composite operators”) built solely from the basic fields θ :

$$F(x) = \theta^n(x). \quad (6.19)$$

In general, a local composite operator is a polynomial constructed from the primary fields $\Phi(x)$ and their finite-order derivatives at a single space-time point $x = (t, \mathbf{x})$. Due to a coincidence of the field arguments, new UV

divergences arise in the Green functions with such objects [9, 10].

The total canonical dimension of an arbitrary 1-irreducible Green function $\Gamma = \langle F \Phi \dots \Phi \rangle$ that includes one composite operator F and arbitrary number of primary fields Φ (the formal index of UV divergence) is given by the relation

$$d_\Gamma = d_F - \sum_{\Phi} N_\Phi d_\Phi, \quad (6.20)$$

where N_Φ is the number of the field Φ entering Γ , d_Φ is the total canonical dimension of the given field Φ , d_F is the canonical dimension of the operator.

In the process of renormalization operators can mix with each other,

$$F_i = \sum_j Z_{ij} F_j^R, \quad (6.21)$$

and Z_{ij} is the renormalization matrix. But in the simplest case of the operators (6.19) the matrix Z_{ij} is diagonal, i.e., $F(x) = Z_F F^R(x)$. In particular, this means that the critical dimension of the operator is given by the expression (5.35).


Superficial UV divergences, whose removal requires counterterms, can be present only in those functions Γ for which the index of divergence $d_{\Gamma_{N_\Phi}}$ is a non-negative integer. For the operators of the form (6.19) one has $d_F = -n$. Due to the linearity of our model in θ , the number of fields θ in any 1-irreducible function with the operator $F(x)$ cannot exceed their number in the operator itself. Thus, from the analysis of Eq. (6.20) it follows that the superficial divergence can only be present in the 1-irreducible function with $N_\theta = n$ and $N_\Phi = 0$ for all other types of the fields Φ . For this function $\delta_\Gamma = 0$ and the corresponding counterterm takes the form $\theta^n(x)$; hence, the operators in (6.19) are multiplicatively renormalizable, $F(x) = Z_n F^R(x)$.

Let us introduce $\Gamma_n(x; \theta)$: the θ^n term of the expansion in $\theta(x)$ of the generating functional of the 1-irreducible Green functions with one composite operator $F(x)$ and any number of fields θ :

$$\begin{aligned} \Gamma_n(x; \theta) = & \int dx_1 \dots \int dx_n \langle F(x) \theta(x_1) \dots \theta(x_n) \rangle \\ & \times \theta(x_1) \dots \theta(x_n). \end{aligned} \quad (6.22)$$

The renormalization constants Z_n are determined by the requirement that the 1-irreducible functions (6.22) be UV finite in the renormalized theory.

The one-loop approximation for the 1-irreducible function $\Gamma_n(x; \theta)$ can be formally written as

$$\Gamma_n(x; \theta) = F(x) + \frac{1}{2} \cdot \text{diagram} \quad (6.23)$$


The first term in Eq. (6.23) is the tree (loop-less) approximation, the double solid lines with a slash denotes the propagators $\langle\theta\theta'\rangle$, the single solid line corresponds to the propagator $\langle vv\rangle$, $1/2$ is the symmetry coefficient of the given graph, and the dot with two attached lines in the top of the diagram denotes the operator vertex, i.e., the variational derivative

$$\begin{aligned} V(x; x_1, x_2) &= \delta^2 F(x) / \delta\theta(x_1) \delta\theta(x_2) \\ &= n(n-1) \theta^{n-2}(x) \delta(x-x_1) \delta(x-x_2). \end{aligned} \quad (6.24)$$

A contribution of a specific diagram into the functional (6.23) for any composite operator F is represented in the form

$$\Gamma_n = V \times I \times \theta \dots \theta, \quad (6.25)$$

where V is the vertex factor given by Eq. (6.24), I is the diagram itself, and the product $\theta \dots \theta$ corresponds to the external tails.

The renormalization constants Z_n are found from the requirement that the renormalized analog $\Gamma_n^R = Z_n^{-1} \Gamma_n$ of the function (6.22) be UV finite in terms of renormalized parameters and take a form

$$Z_n = 1 + \frac{n(n-1)}{4wu(u+w)} \left(\frac{\alpha g_1}{y} + \frac{g_2}{\varepsilon} \right); \quad (6.26)$$

see Appendix B 2 for details. The corresponding anomalous dimensions are

$$\gamma_n = -\frac{n(n-1)}{4wu(u+w)} (\alpha g_1 + g_2), \quad (6.27)$$

with higher-order corrections in g_1 and g_2 .

The critical dimensions of the operators θ^n from the expression (5.35) are readily derived

$$\Delta[\theta^n] = n\Delta_\theta + \gamma_n^*. \quad (6.28)$$

Substituting the fixed-point values FP II and FP III into Eq. (6.27) finally gives the critical dimensions

$$\Delta[\theta^n] = -n + \frac{n\varepsilon}{4} - \frac{n(n-1)}{3}\varepsilon \quad (6.29)$$

for the point FP II;

$$\Delta[\theta^n] = -n + \frac{ny}{6} - \frac{2n(n-1)}{3} \frac{\alpha y(y-\varepsilon)}{y(\alpha+2) - 3\varepsilon} \quad (6.30)$$

for the point FP III. Both the expressions (6.29) and (6.30) assume higher-order corrections in y and ε . For both cases, FP II and FP III, the dimensions are negative, i.e., “dangerous” in the sense of operator product expansion [9, 14], and decrease as n grows.

The latter result for FP III is in agreement with previously known result [38] for the analysis near three-dimensional space $d = 3$:

$$\Delta[\theta^n] = -n + \frac{ny}{6} - \frac{n(n-1)}{6} \frac{\alpha dy}{(d-1)}, \quad (6.31)$$

which at $d = 4$ reads

$$\Delta[\theta^n] \Big|_{d=4} = -n + \frac{ny}{6} - \frac{2\alpha y}{9} n(n-1). \quad (6.32)$$

Expanding the expression (6.30) in y at fixed (not small) value $\varepsilon = 1$ (which corresponds to $d = 3$) gives

$$\Delta[\theta^n] = -n + \frac{ny}{6} - \frac{2\alpha y}{9} n(n-1) + \mathcal{O}(y^2). \quad (6.33)$$

From the expressions (6.32) and (6.33) it follows that the expression (6.30), obtained as a result of the double y and ε expansion near $d = 4$, may be considered as a certain partial infinite resummation of the ordinary y expansion. This resummation significantly improves the situation at large α – now we do not have the pathology when the critical dimensions $\Delta[\theta^n]$ grow with α without a bound and also that the fixed point ceases to exist at the single value $\alpha = \infty$.

E. Operator product expansion and anomalous scaling

The measurable quantities and, therefore, the objects of interest are equal-time pair correlation functions of two (UV finite) renormalized local composite operators $F_{1,2}(x)$. From the dimensional considerations (see Table I) it follows that

$$\langle F_1(t, \mathbf{x}_1) F_2(t, \mathbf{x}_2) \rangle = \nu^{d_F^\omega} \mu^{d_F} f(\mu r, mr, c/\mu\nu),$$

where d_F^ω and d_F are the frequency and total canonical dimensions of the correlation function, $r = |\mathbf{x}_2 - \mathbf{x}_1|$, and f is a function of dimensionless variables.

If the correlation function (6.34) is multiplicatively renormalizable, in the IR region it fulfills the differential equation (5.34), which describes the IR scaling behavior. That is, the behavior of the function f for $\mu r \gg 1$ is determined by the IR attractive fixed points FP II and FP III of the RG equation. A solution of this equation leads to the following asymptotic expression:

$$\langle F_1(t, \mathbf{x}_1) F_2(t, \mathbf{x}_2) \rangle \simeq \nu^{d_F^\omega} \mu^{d_F} (\mu r)^{-\Delta_F} h[mr, \bar{c}(r)]. \quad (6.34)$$

Here, Δ_F is the critical dimension of the correlation function, given by a simple sum of the dimensions of the operators; h is an unknown scaling function with completely (both canonically and critically) dimensionless arguments, and $\bar{c}(r)$ is invariant speed of sound.

For the composite operator $F(x) = \theta^n(x)$, Eq. (6.34) yields

$$\langle \theta^p(t, \mathbf{x}_1) \theta^k(t, \mathbf{x}_2) \rangle \simeq \mu^{-(p+k)} (\mu r)^{-\Delta_p - \Delta_k} h_{pk}[mr, \bar{c}(r)], \quad (6.35)$$

where the critical dimensions Δ_n for two scaling regimes are given by Eqs. (6.29) and (6.30).

The representation (6.35) holds for $\mu r \gg 1$ and any fixed value of mr . The inertial-convective range

$l \ll r \ll \mathcal{L}$ corresponds to the additional condition $mr \ll 1$. Behavior of the function h at $mr \rightarrow 0$ can be studied by means of the operator product expansion; see [9, 10]. According to the OPE, the equal-time product $F_1(x_1)F_2(x_2)$ of two renormalized operators for $\mathbf{x} \equiv (\mathbf{x}_1 + \mathbf{x}_2)/2 = \text{const}$ and $\mathbf{r} \equiv \mathbf{x}_1 - \mathbf{x}_2 \rightarrow 0$ takes the form

$$F_1(t, \mathbf{x}_1)F_2(t, \mathbf{x}_2) \simeq \sum_F C_F[mr, \bar{c}(r)]F(t, \mathbf{x}), \quad (6.36)$$

where C_F are numerical coefficient functions analytical in mr and $\bar{c}(r)$ and F are all possible renormalized local composite operators allowed by the symmetry.

The correlation function (6.34) is obtained by averaging (6.36) with the weight $\exp \mathcal{S}_R$, where \mathcal{S}_R is the renormalized action functional (6.3). Mean values $\langle F(x) \rangle \propto (mr)^{\Delta_F}$ appear in the right hand side. Their asymptotic behavior at small m is found from the corresponding RG equations and takes the form

$$\langle F(x) \rangle \simeq m^{\Delta_F} q[\bar{c}(1/m)], \quad (6.37)$$

with another set of scaling functions q . Since the diagrams of the perturbation theory have finite limits both for $c \rightarrow \infty$ and $c \rightarrow 0$, we may assume that the functions $q(c)$ are restricted for all values of c and can be estimated by some constants. Moreover, for the invariant variable $\bar{c}(r)$ IR asymptotic behavior together with requirement of its dimensionless gives

$$\bar{c}(r) = c(\mu r)^{\Delta_c} / (\mu \nu), \quad (6.38)$$

where c is renormalized speed of sound. Thus, $\bar{c}(1/m) \sim cm^{-\Delta_c}$. Taking into account (5.37), for the non-local scaling regime FPIII one obtains that for $y > 12/5$ (i.e., including the most realistic case $y \rightarrow 4$) the argument $cm^{-\Delta_c}$ becomes small for fixed c and $m \rightarrow 0$, and the function q can be replaced by its finite limit value $q(0)$. For the local scaling regime FPII from (5.36) it follows that as $\varepsilon \rightarrow 1$ the function q can be replaced by its finite limit value $q(\infty)$. From these two remarks we conclude that in the IR range for both the local and non-local scaling regimes up to a different constants we can write

$$\langle F(x) \rangle \sim m^{\Delta_F}. \quad (6.39)$$

Combining the RG representation (6.35) with the information gained from the OPE (6.36) and Eq. (6.39) gives the desired asymptotic behavior of the scaling functions

$$h[mr, c(r)] \simeq \sum_F A_F[mr, c(r)] (mr)^{\Delta_F}, \quad (6.40)$$

where the summation runs over all the Galilean invariant scalar operators (including operators with derivatives, etc.), with the coefficient functions A_F analytical in their arguments. The leading contribution in the sum (6.40) is given by the operator with the lowest (minimal) critical

dimension; others can be considered as corrections. The anomalous scaling (i.e., singular behavior as $mr \rightarrow 0$) results from the contributions of the operators with negative critical dimensions. From (6.29) and (6.30) it is easily seen that for both scaling regimes all the operators θ^n have negative dimensions, and the spectrum of their dimensions is not restricted from below.

Fortunately, due to the linearity of the initial stochastic equation (6.1) in the field θ , the number of such fields in the right hand side of the expression (6.36) cannot exceed their number in the left hand side. Thus, for a given correlation function only a finite number of those operators can contribute to the OPE. For the correlation functions (6.35) these operators are those for which $n \leq p + k$. The leading term of the behavior as $mr \rightarrow 0$ is given by the operator with the maximum possible $n = p + k$ and without any derivatives, so the final expression takes the form

$$\langle \theta^p(t, \mathbf{x}_1) \theta^k(t, \mathbf{x}_2) \rangle \simeq \mu^{-(p+k)} (\mu r)^{-\Delta_p - \Delta_k} (mr)^{\Delta_{p+k}}. \quad (6.41)$$

The fact that the leading term in the OPE is given by the operator from the same family with the summed exponent together with inequality $\Delta_p + \Delta_k > \Delta_{p+k}$ can be interpreted as the statement that the correlations of the scalar field in the model (6.1) show multi-fractal behavior; see [68].

VII. CONCLUSION

In this paper, which is an extension of [38, 55], the stochastic Navier-Stokes equation for a compressible fluid was studied using the field theoretic approach. In contrast to previous studies, we analyzed the model near the special space dimension $d = 4$, where the model possesses an additional UV divergence in the 1-irreducible Green function $\langle v'_i v'_j \rangle$. This feature significantly affects both technical aspects and results of the RG analysis. In particular, it necessitates the renormalization group technique with a double expansion scheme. In the one-loop approximation, the model possesses two attractive non-trivial fixed points in the IR region, i.e., two possible non-trivial scaling regimes – a local one, denoted FPII in the text, and a non-local one, FPIII. These points depend on the exponent y and on $\varepsilon = 4 - d$, the deviation of the space dimension d from its special value 4.

Analysis at $d = 3$, which finds only one non-trivial fixed point corresponding to the non-local scaling regime [38, 55] should therefore be regarded as incomplete. The crossover between the local and non-local regimes occurs along the line $y = 3\varepsilon/2$, which is in accordance with [37]. The new (local) regime, which arises at $d = 4$, continuously moves to $d = 3$ as $\varepsilon \rightarrow 1$. Nevertheless, the quantitative RG analysis, based on the one-loop approximation, shows that for the real values of the parameters $y = 4$ and $\varepsilon = 1$ the new local point FPII is not IR attractive, but the non-local point FPIII is. This

finding confirms the RG analysis in [38, 55], done within the single expansion in y . However, the situation may change at the two-loop level, where, for example, the areas of stability of two different fixed points may overlap and the choice of fixed point, which defines asymptotic behavior, will depend on the initial data g_{10}, g_{20}, u_0, v_0 , and w_0 . Herewith, the local point FPII describes the system near thermal equilibrium and is valid (IR attractive) for all y and ε if the pumping of energy by large-scale eddies is absent, i.e., if $g_{10} = 0$.

We also analyzed the model of passive scalar advection of density field by this velocity ensemble. The full stochastic problem can be formulated as a field theoretic model, which is multiplicatively renormalizable. The new parameter κ does not affect the RG functions of the Navier-Stokes equation itself, so the critical behavior of this model is also described by two fixed points, a local one and non-local one. The inertial range ($l \ll r \ll \mathcal{L}$) behavior of correlation functions was studied using the OPE technique. The existence of anomalous scaling, i.e., singular power-like dependence on the integral scale \mathcal{L} , was established. The corresponding anomalous exponents were identified with critical dimensions of certain composite operators and calculated in the leading one-loop approximation.

The results of this study are especially significant at large values of α (purely potential random force). In contrast to analysis near $d = 3$, in the present case the anomalous dimensions of the composite operators (6.29) and (6.30) do not grow with α without a bound. This is a consequence of eliminating the poles in ε near $d = 4$, which leads to a significant improvement of calculated expressions for critical dimensions near physical value $d = 3$. A previous study [38] suggested that the real expansion parameter is αy rather than y , therefore, any finite order of this (αy) expansion is not suitable for studying the behavior at large α . According to this observation, it is necessary to perform a resummation assuming that y is small and $\alpha y \sim 1$. Expression (6.30) obtained in this study provides an example of such resummation. It works well at large α being not expanded in y , and the first term of this expansion coincides with the answer presented in [38]; see the expressions (6.32) – (6.33). The hypothesis that the scaling regimes undergo a qualitative changeover, possibly accompanied by phase transition to a purely chaotic state, was presented in previous study [55] based on the observation that for some large value of α the points FPII and FPIII disappear or lose their stability. From the expression (6.30) it follows that this hypothesis is not confirmed. The consideration of the present model near $d = 4$ is similar to the RG analysis of the Navier-Stokes equation for incompressible fluid near $d = 2$, where additional renormalization near the special space dimension $d = 2$ improves the agreement of the predicted Kolmogorov constant with experimental results [60].

Double y and ε expansion near $d = 4$ provides an additional interesting opportunity – it allows to analyze

whether a non-local fixed point is a node or a spiral attractor. The anomalous exponents do not depend on the type of attractor, but the behavior of the RG flow is interesting itself. Depending on the values of the parameters y and ε the point FPIII might be a spiral attractor if $\alpha > \frac{1}{5}(-7 + 3\sqrt{6}) \approx 0.07$. At their physically relevant values, i.e., $y = 4$ and $\varepsilon = 1$, the point FPIII becomes a spiral attractor if $\alpha > \frac{5}{176}(-26 + 9\sqrt{15}) \approx 0.25$.

It would be very interesting to go beyond the one-loop approximation and to examine the existence, stability and α -dependence of fixed points at the two-loop level, which seems to be a technically difficult task. In addition, it would be very interesting to investigate scalar admixture in the case of a tracer field or passively advected vector fields. Another very important task is to develop the compressible Navier-Stokes equation near $d = 2$. Such analysis may reveal additional types of IR behavior or another dependence on parameters like α , viscosity ratios, etc. These studies are underway and are left for the future.

ACKNOWLEDGMENTS

The authors are indebted to Loran Ts. Adzhemyan, Michal Hnatič, Juha Honkonen, Mikhail V. Kompaniets, Nikita M. Lebedev, Mikhail Yu. Nalimov, and Viktor Škultéty for discussions and Maria, John, and Aviva Bloom for reading the manuscript.

The work was supported by VEGA grant No. 1/0345/17 of the Ministry of Education, Science, Research and Sport of the Slovak Republic, by the Russian Foundation for Basic Research within the Project 16-32-00086, and by the Ministry of Education and Science of Russian Federation (the Agreement number 02.a03.21.0008). N. M. G. acknowledges the support from the Saint Petersburg Committee of Science and High School. N. M. G. and M. M. K. were also supported by Dmitry Zimin's Dynasty Foundation.

Appendix A: Calculation of the diagrams for Navier-Stokes stochastic equation

This section contains detailed calculations of the diagrams, defining the renormalization constants $Z_1 - Z_6$ (see Sec. IV A). All calculations are performed in the analytical regularization and the MS scheme. All diagrams are calculated in arbitrary space dimension d , and only poles in y and $\varepsilon = 4 - d$ are presented in the results. The renormalization constants obtained this way do not depend on the parameter $c_0 \sim c$, so that it is possible to set $c_0 = 0$ in the propagators [see (3.4)] in all the cases, in which some quantity is not proportional to c_0 . If some quantity is proportional to c_0 , we may set $c_0 = 0$ after we have obtained the needed power of it. This means that we may set $c_0 = 0$ in all denominators, preserving them in numerators. The situation is similar to calculations of

critical exponents in models of critical behavior, which can be performed in the “massless” models: we may consider c_0 to play a similar role as $\tau \propto T - T_c$ in ϕ^4 model.

In the MS scheme, the renormalization constants do not depend on τ and can be calculated directly at the critical point $\tau = 0$; see [9, 55].

1. The diagram with $d_\Gamma = 0$

Start with the simplest graph for which $d_\Gamma = 0$ and which appears in Eq. (4.6):

$$D_1 = \text{---} \overbrace{\text{---}}^{\text{---}} \text{---} \quad (\text{A1})$$

The corresponding analytical expression reads

$$\begin{aligned} D_1 &= (-i)^2 \int \frac{d\omega}{2\pi} \int \frac{d^d \mathbf{k}}{(2\pi)^d} (k_b \delta_{ia} - k_a \delta_{bi})(k_c \delta_{jd} - k_d \delta_{jc}) \\ &\times \left[P_{ac}(\mathbf{k}) \frac{g_{10} \nu_0^3 k^{4-d-y} + g_{20} \nu_0^3}{|\epsilon_1(k)|^2} + Q_{ac}(\mathbf{k}) (\alpha g_{10} \nu_0^3 k^{4-d-y} + g_{20} \nu_0^3) \left| \frac{\epsilon_3(k)}{R(k)} \right|^2 \right] \\ &\times \left[P_{bd}(\mathbf{k}) \frac{g_{10} \nu_0^3 k^{4-d-y} + g_{20} \nu_0^3}{|\epsilon_1(k)|^2} + Q_{bd}(\mathbf{k}) (\alpha g_{10} \nu_0^3 k^{4-d-y} + g_{20} \nu_0^3) \left| \frac{\epsilon_3(k)}{R(k)} \right|^2 \right]; \end{aligned} \quad (\text{A2})$$

hereinafter the Roman letters i and j are external (free) indices of the diagram, while the Roman letters a, \dots, d denote the vector indices of the propagators with the implied summation over repeated indices. Two terms in the first line are vertices V_{ijl}^1 (see Fig. 2), terms in the second and the third line are propagators $\langle v_i v_j \rangle$, see (3.4) and (3.6). Since $d_\Gamma = 0$ for this diagram, we may put the external momenta $\mathbf{p} = 0$.

The calculation of the tensor structure J_{ij}^1 gives

$$J_{ij}^1 = 2(-\delta_{ij} k^2 + k_i k_j) A(k) B(k), \quad (\text{A3})$$

where $A(k)$ and $B(k)$ are the scalar parts of the propagators in the expression (A2), namely,

$$\begin{aligned} A(k) &= \frac{g_{10} \nu_0^3 k^{4-d-y} + g_{20} \nu_0^3}{|\epsilon_1(k)|^2}; \\ B(k) &= (\alpha g_{10} \nu_0^3 k^{4-d-y} + g_{20} \nu_0^3) \left| \frac{\epsilon_3(k)}{R(k)} \right|^2. \end{aligned} \quad (\text{A4})$$

The integration over the frequency ω of the expression (A3) gives

$$\int \frac{d\omega}{2\pi} A(k) B(k) = \frac{1}{2k^6 \nu_0^3 u_0 (u_0 + 1)}, \quad (\text{A5})$$

therefore, the expression (A2) takes the form

$$\begin{aligned} D_1 &= \int \frac{d^d \mathbf{k}}{(2\pi)^d} \frac{\nu_0^3}{u_0 (u_0 + 1)} \frac{1}{k^4} \left(\delta_{ij} - \frac{k_i k_j}{k^2} \right) \\ &\times (g_{10} k^{4-d-y} + g_{20}) (\alpha g_{10} k^{4-d-y} + g_{20}). \end{aligned} \quad (\text{A6})$$

In order to integrate over the vector \mathbf{k} we need to average the expression (A6) over the angle variables:

$$\int d^d \mathbf{k} f(\mathbf{k}) = S_d \int_0^\infty dk k^{d-1} \langle f(\mathbf{k}) \rangle, \quad (\text{A7})$$

where $\langle \dots \rangle$ is the averaging over the unit sphere in the d -dimensional space, $S_d = 2\pi^{d/2}/\Gamma(d/2)$ is its surface area. To perform an averaging of a given function of \mathbf{k} over the angle variables we use the relations

$$\left\langle \frac{k_i k_j}{k^2} \right\rangle = \frac{\delta_{ij}}{d}, \quad (\text{A8})$$

$$\left\langle \frac{k_i k_j k_l k_m}{k^4} \right\rangle = \frac{\delta_{ij} \delta_{lm} + \delta_{il} \delta_{jm} + \delta_{im} \delta_{jl}}{d(d+2)}. \quad (\text{A9})$$

In particular, Eq. (A8) means that

$$\int d^d \mathbf{k} \frac{k_i k_s}{k^2} f(k) = \frac{\delta_{is}}{d} \int d^d \mathbf{k} f(k). \quad (\text{A10})$$

For D_1 this yields

$$\begin{aligned} D_1 &= \frac{\nu_0^3}{u_0 (u_0 + 1)} \frac{d-1}{d} \delta_{ij} C_d \int d^d k \frac{k^{d-1}}{k^4} [\alpha g_{10}^2 k^{8-2d-2y} \\ &+ (\alpha + 1) g_{10} g_{20} k^{4-d-y} + g_{20}^2], \end{aligned} \quad (\text{A11})$$

where $C_d = S_d/(2\pi)^d$. After the angular averaging has been performed, we are left with simple integrals over the modulus k :

$$\begin{aligned} \int_m^\infty d^d k k^{d-1} \frac{k^{4-d-y}}{k^4} &= \frac{m^{-y}}{y}; \\ \int_m^\infty d^d k k^{d-1} \frac{1}{k^4} &= \frac{m^{-\varepsilon}}{\varepsilon}, \end{aligned} \quad (\text{A12})$$

where $\varepsilon = 4-d$. Applying these expressions to Eq. (A11), one obtains

$$D_1 = \frac{\nu_0^3}{u_0(u_0 + 1)} \frac{d-1}{d} \delta_{ij} C_d \left[\frac{\alpha g_{10}^2}{2y - \varepsilon} + \frac{(\alpha + 1)g_{10}g_{20}}{y} + \frac{g_{20}^2}{\varepsilon} \right]. \quad (\text{A13})$$

Taking into account the symmetry coefficient 1/2 for this graph, Eq. (4.6) finally reads

$$\begin{aligned} \Gamma_{v'v'} &= g_{10}\nu_0^3\mu^y p^{4-d-y} \left\{ P_{ij}(\mathbf{p}) + \alpha Q_{ij}(\mathbf{p}) \right\} + Z_6 g_{20}\nu_0^3 \delta_{ij} \\ &+ \frac{\nu_0^3}{u_0(u_0 + 1)} \frac{d-1}{2d} \delta_{ij} C_d \left[\alpha g_{10}^2 \frac{m^{\varepsilon-2y}}{2y - \varepsilon} + (\alpha + 1)g_{10}g_{20} \frac{m^{-y}}{y} + g_{20}^2 \frac{m^{-\varepsilon}}{\varepsilon} \right]. \end{aligned} \quad (\text{A14})$$

2. The diagrams with $d_\Gamma = 1$

In this section we discuss now linearly divergent diagrams. We begin with one of the diagrams, entering the

expansion of the function $\langle \phi'v \rangle$ [see (4.5)], namely,

$$D_2 = \text{---} \overbrace{\text{---}}^{\text{---}} \text{---}. \quad (\text{A15})$$

In the frequency-momentum representation it is given by

$$\begin{aligned} D_2 &= \int \frac{d\omega}{2\pi} \int \frac{d^d \mathbf{k}}{(2\pi)^d} V_b(\mathbf{p} + \mathbf{k}) V_j(\mathbf{k}) \langle \phi \phi' \rangle(p + k) \langle v_b \phi \rangle^*(\mathbf{k}) \\ &= ic_0^2 \nu_0^3 \int \frac{d\omega}{2\pi} \int \frac{d^d \mathbf{k}}{(2\pi)^d} [k^2 + (\mathbf{p} \cdot \mathbf{k})] k_j \frac{\alpha g_{10} k^{4-d-y} + g_{20}}{\varepsilon_2(k) \varepsilon_3(k) \varepsilon_3(p+k) \varepsilon_2^*(k)}, \end{aligned} \quad (\text{A16})$$

where both $V_b(\mathbf{p} + \mathbf{k})$ and $V_j(\mathbf{k})$ are interaction vertices (see Fig. 2), $\langle \phi \phi' \rangle$ and $\langle v_b \phi \rangle^*$ are two propagators, see (3.4); \mathbf{p} is an external momenta, \mathbf{k} – internal one; $(\mathbf{p} \cdot \mathbf{k})$ denotes the scalar product of vectors \mathbf{p} and \mathbf{k} .

Since this diagram is linearly divergent, $d_\Gamma = 1$, only the terms proportional to \mathbf{p} need to be computed. An integration of the scalar part in Eq. (A16) over the frequency and an expansion of the result up to first order in \mathbf{p} gives

$$\begin{aligned} &\int \frac{d\omega}{2\pi} \frac{1}{\varepsilon_2(k) \varepsilon_3(k) \varepsilon_3(p+k) \varepsilon_2^*(k)} \\ &\cong \frac{1}{2u_0(u_0 + v_0)^2 \nu_0^3} \frac{1}{k^4} \left[\frac{1}{k^2} - \frac{2v_0(\mathbf{p} \cdot \mathbf{k})}{k^4(u_0 + v_0)} \right]. \end{aligned} \quad (\text{A17})$$

Substituting this expression into Eq. (A16) and performing averaging over the angles [see Eq. (A9)] one obtains

$$\begin{aligned} D_2 &= p_j \frac{1}{d} \frac{ic_0^2}{2u_0(u_0 + v_0)^2} \left(1 - \frac{2v_0}{u_0 + v_0} \right) C_d \\ &\times \int k^{d-1} d^d k \frac{1}{k^4} (\alpha g_{10} k^{4-d-y} + g_{20}). \end{aligned} \quad (\text{A18})$$

Finally, use of Eq. (A12) leads to the following result:

$$D_2 = ic_0^2 p_j \frac{1}{d} \frac{u_0 - v_0}{2u_0(u_0 + v_0)^3} C_d$$

$$\times \left(\alpha g_{10} \frac{m^{-y}}{y} + g_{20} \frac{m^{-\varepsilon}}{\varepsilon} \right). \quad (\text{A19})$$

The second diagram, entering the expansion of the function $\langle \phi'v \rangle$, is

$$D_3 = \text{---} \overbrace{\text{---}}^{\text{---}} \text{---}. \quad (\text{A20})$$

The analytical expression for the diagram reads

$$\begin{aligned} D_3 &= \int \frac{d\omega}{2\pi} \int \frac{d^d \mathbf{k}}{(2\pi)^d} V_a(\mathbf{k} + \mathbf{p}) V_{dcj} \\ &\times \langle v_a v_c \rangle(\mathbf{k}) \langle \phi v'_d \rangle(\mathbf{p} + \mathbf{k}), \end{aligned} \quad (\text{A21})$$

where V_{dcj} and $V_a(\mathbf{k} + \mathbf{p})$ are two vertices, $\langle v_a v_c \rangle$ and $\langle \phi v'_d \rangle$ are two propagators.

The tensor structure J_j^3 for this diagram is

$$\begin{aligned} J_j^3 &= (-1)^2 (k + p)_a (k_j \delta_{cd} + p_c \delta_{dj}) (k + p)_d \\ &\times [P_{ac}(\mathbf{k}) A(k) + Q_{ac}(\mathbf{k}) B(k)], \end{aligned} \quad (\text{A22})$$

where $A(k)$ and $B(k)$ are scalar coefficients from Eq. (A4). After summation over vector indices up to the first order in \mathbf{p} one obtains

$$J_j^3 \cong k_j [k^2 + 3(\mathbf{p} \cdot \mathbf{k})] B(k). \quad (\text{A23})$$

Since we have put $c_0 = 0$ in all denominators, an integration over frequency and an expansion of obtained

expression up to first order in \mathbf{p} yields

$$\begin{aligned} & \int \frac{d\omega}{2\pi} \frac{B(k)}{R(p+k)} = \int \frac{d\omega}{2\pi} \frac{1}{|\epsilon_2(k)|^2 R(p+k)} \\ &= \frac{1}{4\nu_0^3 u_0^2 (u_0 + v_0) k^6} \left[1 - \frac{u_0 + 3v_0}{u_0 + v_0} \frac{(\mathbf{p} \cdot \mathbf{k})}{k^2} \right]. \end{aligned} \quad (\text{A24})$$

Combining Eqs. (A23) and (A24), averaging the obtained result over angle variables, and applying Eq. (A12) one obtains

$$\begin{aligned} D_3 &= ic_0^2 p_j \frac{1}{d} \frac{1}{2u_0(u_0 + v_0)^2} C_d \\ &\times \left(\alpha g_{10} \frac{m^{-y}}{y} + g_{20} \frac{m^{-\varepsilon}}{\varepsilon} \right). \end{aligned} \quad (\text{A25})$$

The last diagram, entering the expansion of the function $\langle \phi' v_j \rangle$, is

$$D_4 = \text{---} \begin{array}{c} \frown \\ \text{---} \\ \smile \end{array} \text{---}. \quad (\text{A26})$$

The analytical expression for it is

$$\begin{aligned} D_4 &= \int \frac{d\omega}{2\pi} \int \frac{d^d \mathbf{k}}{(2\pi)^d} V_a(\mathbf{k}) V_{dcj} \\ &\times \langle v_d \phi \rangle(\mathbf{k}) \langle v_a v'_c \rangle(\mathbf{p} + \mathbf{k}), \end{aligned} \quad (\text{A27})$$

where V_{dcj} and $V_a(\mathbf{k})$ are two vertices, $\langle v_d \phi \rangle$ and $\langle v_a v'_c \rangle$ are two propagators.

The tensor structure J_j^4 for this diagram is

$$\begin{aligned} J_j^4 &= k_a k_c (k_j \delta_{cd} + p_c \delta_{dj}) \\ &\times [P_{ad}(\mathbf{p} + \mathbf{k}) C(p+k) + Q_{ad}(\mathbf{p} + \mathbf{k}) D(p+k)], \end{aligned} \quad (\text{A28})$$

where $C(p+k)$ and $D(p+k)$ are the scalar coefficients of the propagator $\langle v_a v'_c \rangle$, namely,

$$C(k) = \frac{1}{\epsilon_1(k)}; \quad D(k) = \frac{\epsilon_3(k)}{R(k)}. \quad (\text{A29})$$

After the summation over vector indices up to the first order in \mathbf{p} one obtains

$$J_j^4 \cong k_j [k^2 + (\mathbf{p} \cdot \mathbf{k})] D(p+k). \quad (\text{A30})$$

Integration over the frequency of the scalar part of the expression (A27) gives

$$\begin{aligned} & \int \frac{d\omega}{2\pi} \frac{D(p+k) \epsilon_3(k)}{|R(k)|^2} = \int \frac{d\omega}{2\pi} \frac{1}{\epsilon_2(p+k) |\epsilon_2(k)|^2 \epsilon_3^*(k)} \\ &= \frac{1}{2\nu_0^3 u_0^2 (u_0 + v_0) k^4} \\ &\times \frac{u(\mathbf{p} + \mathbf{k})^2 + k^2 (2u_0 + v_0)}{[k^2 + (\mathbf{p} + \mathbf{k})^2][v_0 k^2 + u_0 (\mathbf{p} + \mathbf{k})^2]}. \end{aligned} \quad (\text{A31})$$

In the same way as it has been done previously we obtain the following result:

$$D_4 = -ic_0^2 p_j \frac{1}{d} \frac{1}{(u_0 + v_0)^3} C_d \left(\alpha g_{10} \frac{m^{-y}}{y} + g_{20} \frac{m^{-\varepsilon}}{\varepsilon} \right). \quad (\text{A32})$$

From Eqs. (A19), (A25) and (A32) it follows that

$$D_2 + D_3 + D_4 = 0 \quad (\text{A33})$$

in the first order in g_1 and g_2 . From this fact we immediately conclude [see (4.5)] that

$$Z_5 = 1. \quad (\text{A34})$$

Unlike the functions $\langle v'_i v_j v_k \rangle$ and, for example, $\langle \phi' v_i v_j \rangle$ (see Sec. III B), the finiteness of the function $\langle \phi' v_j \rangle$ is not because of an internal symmetry of the system, but it is the result of direct calculations, i.e., the result of cancellation of the non-trivial contributions of three diagrams. Therefore, it is unclear whether this result is exact or it is broken in higher orders of the perturbation theory.

The last diagram with $d_\Gamma = 1$ is the diagram, entering the expansion of the function $\langle v'_i \phi \rangle$ [see (4.4)], namely,

$$D_5 = \text{---} \begin{array}{c} \frown \\ \text{---} \\ \smile \end{array} \text{---}. \quad (\text{A35})$$

The analytical expression for it is

$$D_5 = \int \frac{d\omega}{2\pi} \int \frac{d^d \mathbf{k}}{(2\pi)^d} V_{iab} V_c(\mathbf{p}) \langle v_a v_c \rangle(\mathbf{k}) \langle v_b \phi' \rangle(\mathbf{p} + \mathbf{k}), \quad (\text{A36})$$

where V_{iab} and $V_c(\mathbf{p})$ are two vertices, $\langle v_a v_c \rangle$ and $\langle v_b \phi' \rangle$ are two propagators.

The tensor structure J_i^5 for this diagram is

$$\begin{aligned} J_i^5 &= (-i)^3 [k_b \delta_{ia} - (p+k)_a \delta_{ib}] (-p_c) (k+p)_b \\ &\times [P_{ac}(\mathbf{k}) A(k) + Q_{ac}(\mathbf{k}) B(k)], \end{aligned} \quad (\text{A37})$$

where $A(k)$ and $B(k)$ are the scalar coefficients (A4). After the summation over the vector indices, up to the first order in \mathbf{p} one obtains

$$J_i^5 \cong [p_i k^2 - (\mathbf{p} \cdot \mathbf{k}) k_i] A(k). \quad (\text{A38})$$

Since we are interested only in the terms proportional to \mathbf{p} and the expression (A23) does not contain zero order term \mathbf{p}^0 , we may put $\mathbf{p} = 0$ in all denominators; hence, integration over the frequency gives

$$\int \frac{d\omega}{2\pi} \frac{A(k)}{R(k)} = \frac{1}{2\nu_0^3 (u_0 + 1) (v_0 + 1) k^6}. \quad (\text{A39})$$

Finally, using the formulas (A9) and (A12) one obtains the following result:

$$\begin{aligned} D_5 &= -ip_i \frac{d-1}{d} \frac{1}{2(u_0 + 1) (v_0 + 1)} C_d \\ &\times \left(g_{10} \frac{m^{-y}}{y} + g_{20} \frac{m^{-\varepsilon}}{\varepsilon} \right). \end{aligned} \quad (\text{A40})$$

3. The diagrams with $d_\Gamma = 2$

Start with the diagram, entering the expansion for function $\langle \phi \phi' \rangle$ [see (4.3)], namely,

$$D_6 = \text{---} \begin{array}{c} \frown \\ \text{---} \\ \smile \end{array} \text{---}. \quad (\text{A41})$$

The analytical expression for it is

$$D_6 = \int \frac{d\omega}{2\pi} \int \frac{d^d \mathbf{k}}{(2\pi)^d} V_a(\mathbf{p} + \mathbf{k}) V_c(\mathbf{p}) \times \langle \phi \phi' \rangle(p+k) \langle v_a v_c \rangle(\mathbf{k}), \quad (\text{A42})$$

where $V_a(\mathbf{k})$ and $V_c(\mathbf{k})$ are two vertices, $\langle \phi \phi' \rangle$ and $\langle v_a v_c \rangle$ are two propagators.

We are interested in the term, proportional to p^2 , therefore, the tensor structure J^6 for this diagram is

$$J^6 = [p^2 k^2 - (\mathbf{p} \cdot \mathbf{k})^2] A(k) + [(\mathbf{p} \cdot \mathbf{k}) k^2 + (\mathbf{p} \cdot \mathbf{k})^2] B(k), \quad (\text{A43})$$

where $A(k)$ and $B(k)$ are the scalar coefficients (A4). After integration over the frequency with function $1/\epsilon_3(p+k)$, which came from the propagator $\langle \phi \phi' \rangle$, using the formulas (A9) and (A12) one obtains the following expression:

$$D_6 = -\frac{\nu_0}{2d} p^2 C_d \left[\frac{d-1}{1+v_0} \left(g_{10} \frac{m^{-y}}{y} + g_{20} \frac{m^{-\epsilon}}{\epsilon} \right) + \frac{(u_0 - v_0)}{u_0(u_0 + v_0)^2} \left(\alpha g_{10} \frac{m^{-y}}{y} + g_{20} \frac{m^{-\epsilon}}{\epsilon} \right) \right]. \quad (\text{A44})$$

The last diagram D_7 , which enters the expansion of the function $\langle v'_i v'_j \rangle$, namely,

$$D_7 = \text{---} \overbrace{\text{---}}^{\text{---}} \text{---}, \quad (\text{A45})$$

is more complicated – both fields v_i and v'_i are vector fields, therefore, there are two possible structures $p^2 \delta_{ij}$

and $p_i p_j$, which are both quadratic in external momentum; see (4.3). The analytical expression for it is

$$D_7 = \int \frac{d\omega}{2\pi} \int \frac{d^d \mathbf{k}}{(2\pi)^d} V_{iab} V_{jcd} \langle v_a v_c \rangle(\mathbf{k}) \langle v_b v'_d \rangle(\mathbf{p} - \mathbf{k}), \quad (\text{A46})$$

where V_{iab} and V_{jcd} are two vertices V_{ijl}^1 (see Fig. 2), $\langle v_a v_c \rangle$ and $\langle v_b v'_d \rangle$ are two propagators.

Divide the expression (A46) into four parts and calculate them separately:

$$D_7 = \int \frac{d\omega}{2\pi} \int \frac{d^d \mathbf{k}}{(2\pi)^d} [k_b \delta_{ia} + (p-k)_a \delta_{ib}] \times (-p_c \delta_{jd} + k_j \delta_{cd}) (I_1 + I_2 + I_3 + I_4), \quad (\text{A47})$$

where

$$\begin{aligned} I_1 &= P_{ac}(\mathbf{k}) P_{bd}(\mathbf{p} - \mathbf{k}) A(k) C(p - k); \\ I_2 &= P_{ac}(\mathbf{k}) Q_{bd}(\mathbf{p} - \mathbf{k}) A(k) D(p - k); \\ I_3 &= Q_{ac}(\mathbf{k}) P_{bd}(\mathbf{p} - \mathbf{k}) B(k) C(p - k); \\ I_4 &= Q_{ac}(\mathbf{k}) Q_{bd}(\mathbf{p} - \mathbf{k}) B(k) D(p - k); \end{aligned} \quad (\text{A48})$$

see (3.4), (3.6), (A4), and (A29).

After integration over the internal frequency ω , expanding the obtained result in external momentum \mathbf{p} up to second order, averaging it over the angle variables [see (A9)] and integrating over the modulus k [see (A12)] one obtains

$$\hat{I}_1 = \frac{1}{4} \nu_0 C_d \left[p^2 P_{ij}(\mathbf{p}) \frac{1-d}{d+2} - p_i p_j \frac{2(d-1)^2}{d(d+2)} \right] \left(g_{10} \frac{m^{-y}}{y} + g_{20} \frac{m^{-\epsilon}}{\epsilon} \right); \quad (\text{A49})$$

$$\begin{aligned} \hat{I}_2 &= \frac{1}{2(u_0 + 1)} \nu_0 C_d \left[p^2 P_{ij}(\mathbf{p}) \left(\frac{4 + 8u_0}{1 + u_0} \frac{1}{d(d+2)} - \frac{2}{d} \right) + p_i p_j \frac{d-1}{d} \left(1 - \frac{4 + 8u_0}{1 + u_0} \frac{1}{d+2} \right) \right] \\ &\times \left(g_{10} \frac{m^{-y}}{y} + g_{20} \frac{m^{-\epsilon}}{\epsilon} \right); \end{aligned} \quad (\text{A50})$$

$$\hat{I}_3 = \frac{1 - u_0}{2u_0(1 + u_0)^2} \nu_0 C_d \frac{1}{d} P_{ij}(\mathbf{p}) \left(\alpha g_{10} \frac{m^{-y}}{y} + g_{20} \frac{m^{-\epsilon}}{\epsilon} \right); \quad (\text{A51})$$

$$\hat{I}_4 = 0, \quad (\text{A52})$$

where

$$\hat{I}_i = \int \frac{d\omega}{2\pi} \int \frac{d^d \mathbf{k}}{(2\pi)^d} [k_b \delta_{ia} + (p-k)_a \delta_{ib}] (-p_c \delta_{jd} + k_j \delta_{cd}) I_i. \quad (\text{A53})$$

Combination of the expressions (A49) – (A52) together leads to the following result for the diagram D_7 :

$$D_7 = p^2 P_{ij}(\mathbf{p}) I_{\perp} + p_i p_j I_{\parallel}, \quad (\text{A54})$$

where

$$I_{\perp} = -\frac{\nu_0 C_d}{2d(1+u_0)^2} \left[\frac{u_0^2 d(d-1) + u_0(2d^2 + 2d - 8) + d(d+3)}{2(d+2)} \left(g_{10} \frac{m^{-y}}{y} + g_{20} \frac{m^{-\varepsilon}}{\varepsilon} \right) + \frac{(u_0 - 1)}{u_0} \left(\alpha g_{10} \frac{m^{-y}}{y} + g_{20} \frac{m^{-\varepsilon}}{\varepsilon} \right) \right]; \quad (\text{A55})$$

$$I_{\parallel} = -\frac{\nu_0 C_d}{2d(1+u_0)^2} (d-1) \frac{u_0^2(d-1) + u_0(d+4) + 1}{(d+2)} \left(g_{10} \frac{m^{-y}}{y} + g_{20} \frac{m^{-\varepsilon}}{\varepsilon} \right). \quad (\text{A56})$$

The expressions (A13), (A40), (A44), and (A54) are final answers for divergent parts of all the Green functions, which are needed to renormalize the model. To find renormalization constants it is necessary to put them into the expressions (4.2) – (4.6) and to require their UV finiteness (when they are expressed in new renormalized variables), i.e., finiteness at $y \rightarrow 0$ and $\varepsilon \rightarrow 0$.

4. Renormalization constants $Z_1 - Z_6$

From the expressions (4.2) and (A54) – (A56) it follows that the renormalization constant Z_1 is connected to the expression I_{\perp} , while the renormalization constant Z_2 is connected to the expression I_{\parallel} . Moreover, one should not forget all the factors like u_0 , v_0 or $g_{1/2,0}$, which are presented in the terms of the action functional and are not necessary presented in the results of calculations of diagrams; see, for example, expression (A14) – not all the terms in the expression (A13) are proportional to the coupling constant g_{20} . In the one-loop approximation we may always replace the bare couplings $g_{1/2,0}$ by their renormalized counterparts $g_{1/2}$: since we have already singled out poles in y and ε , taking into account corrections $Z_{g_{1/2}}$ would be an excess of accuracy; see, e.g., (A19). The multipliers like $(m/\mu)^y$, which are connected with $Z_{g_{1/2}}$, in the MS scheme are equal to 1. This observation also takes place for all other parameters, namely u , v , ν , and c . Passing to new variables according to the convention $g_{1,2} \rightarrow g_{1,2} C_d$ one finally obtains

$$\begin{aligned} Z_1 &= 1 - \frac{u^2 d(d-1) + u(2d^2 + 2d - 8) + d(d+3)}{4d(d+2)(1+u)^2} \\ &\quad \times \left(\frac{g_1}{y} + \frac{g_2}{\varepsilon} \right) - \frac{u-1}{2du(1+u)^2} \left(\alpha \frac{g_1}{y} + \frac{g_2}{\varepsilon} \right); \\ Z_2 &= 1 - (d-1) \frac{u^2(d-1) + u(d+4) + 1}{2d(d+2)u(1+u)^2} \left(\frac{g_1}{y} + \frac{g_2}{\varepsilon} \right); \\ Z_3 &= 1 - \frac{1}{2dv} \left[\frac{d-1}{v+1} \left(\frac{g_1}{y} + \frac{g_2}{\varepsilon} \right) + \frac{(u-v)}{u(u+v)^2} \left(\alpha \frac{g_1}{y} + \frac{g_2}{\varepsilon} \right) \right]; \\ Z_4 &= 1 + \frac{d-1}{2d(1+u)(1+v)} \left(\frac{g_1}{y} + \frac{g_2}{\varepsilon} \right); \end{aligned}$$

$$Z_6 = 1 - \frac{d-1}{2du(1+u)} \left[\alpha \frac{g_1^2}{g_2(2y-\varepsilon)} + (\alpha+1) \frac{g_1}{y} + \frac{g_2}{\varepsilon} \right]. \quad (\text{A57})$$

As it was mentioned in (A34), the renormalization constant Z_5 is trivial.

To find renormalization constants Z for the fields ϕ and ϕ' and physical parameters of the system one should use the relations (4.7) and the binomial relation $(1+x)^{-n} = 1 - nx + \mathcal{O}(x^2)$, which is necessary to calculate Z_i^{-n} .

Appendix B: Calculation of the diagrams for advection-diffusion stochastic equation

In this section the detailed calculations of the diagrams, defining the renormalization constants Z_{κ} (see Sec. VIC) and Z_n (see Sec. VID), are presented.

1. The diagram for response function $\langle \theta' \theta \rangle$

The constant Z_{κ} is to be found from the requirement of UV finiteness of the 1-irreducible Green function $\langle \theta' \theta \rangle$. Like for the original Navier-Stokes model, the divergent part of the considered Feynman diagram is independent on $c_0 \sim c$ and, therefore, can be calculated directly at $c = 0$.

An analytical expression for the diagram D_8 ,

$$D_8 = \text{---} \overbrace{\text{---}}^{\text{---}} \text{---}, \quad (\text{B1})$$

which enters the expression (6.10), is

$$\begin{aligned} D_8 &= \int \frac{d\omega}{2\pi} \int \frac{d^d \mathbf{k}}{(2\pi)^d} V_a(\mathbf{p}) V_c(\mathbf{p} + \mathbf{k}) \frac{1}{-i\omega + w_0 \nu_0 (\mathbf{p} + \mathbf{k})^2} \\ &\quad \times [P_{ac}(\mathbf{k}) A(k) + Q_{ac}(\mathbf{k}) B(k)]. \end{aligned} \quad (\text{B2})$$

Here $V_a(\mathbf{p}) = ip_a$ and $V_c(\mathbf{p} + \mathbf{k}) = i(p+k)_c$ are two vertices of the type (6.6), $w_0 = \nu_0/\kappa_0$; scalar coefficients $A(k)$ and $B(k)$ of the propagator $\langle v_a v_c \rangle$ are defined in (A4).

Since in the leading-order approximation the renormalization constant Z_{κ} in the bare term of (6.10) is taken only in the first order in coupling constants g_1 and g_2 , i.e., $\kappa_0 = \kappa Z_{\kappa} \simeq \kappa(1 + z_y^{(1)} g_1/y + z_{\varepsilon}^{(1)} g_2/\varepsilon)$, during the actual calculation all other renormalization constants in the diagram D_8 , entering, for example, the functions $A(k)$ and $B(k)$, should be replaced with unities.

From the integration over the frequency we get

$$\int \frac{d\omega}{2\pi} \frac{A(k)}{-i\omega + w\nu(\mathbf{p} + \mathbf{k})^2} = \frac{1}{2\nu^2 k^2 [k^2 + w(\mathbf{p} + \mathbf{k})^2]};$$

$$\int \frac{d\omega}{2\pi} \frac{B(k)}{-i\omega + w\nu(\mathbf{p} + \mathbf{k})^2} = \frac{1}{2\nu^2 u k^2 [uk^2 + w(\mathbf{p} + \mathbf{k})^2]}.$$
(B3)

The expression (B2) can be separated into two parts:

$$\check{I}_1 = - \int \frac{d^d \mathbf{k}}{(2\pi)^d} p_a(p+k)_c \frac{P_{ac}(\mathbf{k})}{2\nu^2 k^2 [k^2 + w(\mathbf{p} + \mathbf{k})^2]};$$

$$\check{I}_2 = - \int \frac{d^d \mathbf{k}}{(2\pi)^d} p_a(p+k)_c \frac{Q_{ac}(\mathbf{k})}{2\nu^2 u k^2 [uk^2 + w(\mathbf{p} + \mathbf{k})^2]}.$$

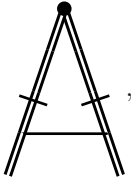
$$D_8 = -p^2 \frac{\nu}{2} \frac{1}{d} \left[\left(\frac{d-1}{w+1} + \frac{\alpha}{u(u+w)} - 2 \frac{\alpha w}{u(u+w)^2} \right) \left(\frac{\mu}{m} \right)^y \frac{g_1}{y} - \left(\frac{d-1}{w+1} + \frac{1}{u(u+w)} - 2 \frac{w}{u(u+w)^2} \right) \left(\frac{\mu}{m} \right)^\varepsilon \frac{g_2}{\varepsilon} \right].$$
(B7)

Therefore, the renormalization constant Z_κ [see (6.10)] should be chosen as

$$Z_\kappa = 1 - \frac{1}{2dw} \left[\frac{d-1}{w+1} + \frac{\alpha(u-w)}{u(u+w)^2} \right] \frac{g_1}{y} - \frac{1}{2dw} \left[\frac{d-1}{w+1} + \frac{u-w}{u(u+w)^2} \right] \frac{g_2}{\varepsilon}.$$
(B8)

2. The diagram for composite operator $\theta^n(x)$

The divergence of the graph D_9 ,



$$D_9 = \text{Diagram},$$
(B9)

entering into the expansion (6.25), is logarithmic, hence, one might set all the external frequencies and momenta equal to zero. Therefore, the analytical expression of the diagram is given by

$$D_9 = \int \frac{d\omega}{2\pi} \int \frac{d^d \mathbf{k}}{(2\pi)^d} V_a(\mathbf{k}) V_c(-\mathbf{k}) \frac{1}{\omega^2 + w^2 \nu^2 k^4} \times [P_{ac}(\mathbf{k}) A(k) + Q_{ac}(\mathbf{k}) B(k)],$$
(B10)

where $V_a(\mathbf{k})$ and $V_c(-\mathbf{k})$ are two vertices (6.6); scalar coefficients $A(k)$ and $B(k)$ of the propagator $\langle v_a v_c \rangle$ are defined in (A4) with the replacement of original bare parameters to their renormalized counterparts. As $V_a(\mathbf{k}) P_{ac}(\mathbf{k}) = 0$, only the second term in (B10) gives a non-vanishing contribution.

We are interested in the term proportional to p^2 . Therefore, in computation of \check{I}_1 one may immediately set $\mathbf{p} = 0$ and, using the expressions (A9), (A12), and the notation $g_i C_d \rightarrow g_i$, get

$$\check{I}_1 = -p^2 \frac{\nu}{2(w+1)} \frac{d-1}{d} \left(g_1 \frac{m^{-y}}{y} + g_2 \frac{m^{-\varepsilon}}{\varepsilon} \right).$$
(B5)

Using Taylor expansion up to the linear term in p for the second part of (B3) we can rewrite \check{I}_2 in the form

$$\check{I}_2 = -p^2 \frac{\nu}{2u(u+w)} \frac{1}{d} \frac{u-w}{u+w} \left(\alpha g_1 \frac{m^{-y}}{y} + g_2 \frac{m^{-\varepsilon}}{\varepsilon} \right).$$
(B6)

Finally, collecting \check{I}_1 and \check{I}_2 yields

Integration over the frequency gives

$$\int \frac{d\omega}{2\pi} \frac{B(k)}{\omega^2 + w^2 \nu^2 k^4} = \frac{1}{2\nu^3} \frac{1}{uw(u+w)} \frac{1}{k^6}.$$
(B11)

Contracting tensor indices, using (A12), and collecting all the factors the expression (6.23) can be rewritten as follows

$$\Gamma_n(x; \theta) = \theta^n(x) \left\{ 1 + \frac{n(n-1)}{4wu(u+w)} \left[\alpha g_1 \left(\frac{\mu}{m} \right)^y \frac{1}{y} + g_2 \left(\frac{\mu}{m} \right)^\varepsilon \frac{1}{\varepsilon} \right] \right\},$$
(B12)

where the substitution $g_i \rightarrow g_i C_d$ is implied.

The renormalization constants Z_n are found from the requirement that the renormalized analog $\Gamma_n^R = Z_n^{-1} \Gamma_n$ of the function (6.22) be UV finite in terms of renormalized parameters. In contrast to the expressions (4.2) – (4.6), in this case the renormalization constants Z_n do not pertain to some model parameters, but to the Green functions themselves. Hence, using the loop expansion (6.23) one does not find the renormalization constants Z_n , but an inversed one Z_n^{-1} . Taking into account a minus sign in the exponent, from (B12) it follows that in the MS scheme the renormalization constants take a form

$$Z_n = 1 + \frac{n(n-1)}{4wu(u+w)} \left(\frac{\alpha g_1}{y} + \frac{g_2}{\varepsilon} \right).$$
(B13)

-
- [1] A. S. Monin and A. M. Yaglom, *Statistical Fluid Mechanics*, Vol.2 (MIT Press, Cambridge, Mass., 1975).
- [2] U. Frisch, *Turbulence: The Legacy of A. N. Kolmogorov* (Cambridge University Press, Cambridge, 1995).
- [3] M. Holzer and A. Pumir, *Phys. Rev E* **47**, 202 (1993); M. Holzer and E. D. Siggia, *Phys. Fluids* **6**, 1820 (1994).
- [4] A. Pumir, *Phys. Fluids* **6**, 2118 (1994).
- [5] C. Tong and Z. Warhaft, *Phys. Fluids* **6**, 2165 (1994).
- [6] B. I. Shraiman and E. D. Siggia, *C.R. Acad. Sci., Ser. IIa: Sci. Terre Planets* **321**, 279 (1995).
- [7] G. Falkovich, K. Gawędzki, and M. Vergassola, *Rev. Mod. Phys.* **73**, 913 (2001).
- [8] P. L. Sulem, J. D. Fournier, and U. Frisch, *Lecture Notes in Physics*, **104**, 321 (1979).
- [9] A. N. Vasil'ev, *The Field Theoretic Renormalization Group in Critical Behavior Theory and Stochastic Dynamics* (Boca Raton, Chapman Hall/CRC, 2004).
- [10] J. Zinn-Justin, *Quantum Field Theory and Critical Phenomena* (4th edition, Oxford University Press, Oxford, 2002).
- [11] D. J. Amit and V. Martin-Mayor, *Field Theory, the Renormalization Group and Critical Phenomena* (World Scientific, Singapore, 2005).
- [12] U. Täuber, *Critical Dynamics: A Field Theory Approach to Equilibrium and Non-Equilibrium Scaling Behavior* (Cambridge University Press, New York, 2014).
- [13] D. V. Shirkov, *Theor. Math. Phys.*, **40**:3, 785 (1979).
- [14] L. Ts. Adzhemyan, N. V. Antonov, A. N. Vasil'ev: *The Field Theoretic Renormalization Group in Fully Developed Turbulence* (Gordon & Breach, London, 1999).
- [15] M. Hnatič, J. Honkonen, T. Lučivjanský, *Acta Physica Slovaca* **66**, 69 (2016).
- [16] D. I. Kazakov, D. V. Shirkov, *Fortsch. Phys.*, **28**:8-9, 465 (1980).
- [17] N. V. Antonov, *J. Phys. A: Math. Gen.* **39**, 7825 (2006).
- [18] L. Ts. Adzhemyan, N. V. Antonov, and A. N. Vasiliev, *Sov. Phys. JETP* **68**(4), 733 (1989); L. Ts. Adzhemyan, N. V. Antonov, T. L. Kim, *Theor. Math. Phys.* **100**, 1086 (1994).
- [19] N. V. Antonov, *J. Sov. Math.*, **47**(2), 2367 (1989); **54**(3), 873 (1991).
- [20] N. V. Antonov and M. M. Kostenko, *Phys. Rev. E* **92**, 053013 (2015).
- [21] L. Ts. Adzhemyan, N. V. Antonov, and A. N. Vasil'ev, *Phys. Rev. E* **58**, 1823 (1998); *Theor. Math. Phys.* **120**, 1074 (1999).
- [22] R.H. Kraichnan, *Phys. Fluids* **11**, 945 (1968); *Phys. Rev. Lett.* **72**, 1016 (1994); *ibid.* **78**, 4922 (1997).
- [23] K. Gawędzki and A. Kupiainen, *Phys. Rev. Lett.* **75**, 3834 (1995); D. Bernard, K. Gawędzki, and A. Kupiainen, *Phys. Rev. E* **54**, 2564 (1996); M. Chertkov, G. Falkovich, I. Kolokolov, and V. Lebedev, *Phys. Rev. E* **52**, 4924 (1995); M. Chertkov and G. Falkovich, *Phys. Rev. Lett.* **76**, 2706 (1996); A. Pumir, *Europhys. Lett.* **34**, 25 (1996); **37**, 529 (1997); *Phys. Rev. E* **57**, 2914 (1998).
- [24] L. Ts. Adzhemyan, N. V. Antonov, V. A. Barinov, Yu. S. Kabrits, and A. N. Vasil'ev, *Phys. Rev. E* **63**, 025303(R) (2001); *E* **64**, 019901(E) (2001); *E* **64**, 056306 (2001).
- [25] N. V. Antonov, *Phys. Rev. E* **60**, 6691 (1999); L. Ts. Adzhemyan, N. V. Antonov, and J. Honkonen, *Phys. Rev. E* **66**, 036313 (2002).
- [26] N. V. Antonov, A. Lanotte, and A. Mazzino, *Phys. Rev. E* **61**, 6586 (2000); N. V. Antonov, N. M. Gulitskiy, *Theor. Math. Phys.*, **176**(1), 851 (2013).
- [27] L. Ts. Adzhemyan, N. V. Antonov, A. Mazzino, P. Muratore Ginanneschi, and A. V. Runov, *Europhys. Lett.* **55**, 801 (2001); H. Arponen, *Phys. Rev. E*, **79**, 056303 (2009).
- [28] N. V. Antonov, M. Hnatič, J. Honkonen, and M. Jurčičin, *Phys. Rev. E* **68**, 046306 (2003).
- [29] N. V. Antonov, N. M. Gulitskiy, *Lecture Notes in Comp. Science*, **7125/2012**, 128 (2012); *Phys. Rev. E* **85**, 065301(R) (2012); *Phys. Rev. E* **87**, 039902(E) (2013).
- [30] N. V. Antonov and N. M. Gulitskiy, *Phys. Rev. E* **91**, 013002 (2015); *Phys. Rev. E* **92**, 043018 (2015); *AIP Conf. Proc.* **1701**, 100006 (2016); *EPJ Web of Conf.* **108**, 02008 (2016).
- [31] E. Jurčičinova, M. Jurčičin, *J. Phys. A: Math. Theor.*, **45**, 485501 (2012); *Phys. Rev. E* **88**, 011004 (2013).
- [32] L. Ts. Adzhemyan, N. V. Antonov, M. Hnatič, and S. V. Novikov, *Phys. Rev. E* **63**, 016309 (2000).
- [33] M. Hnatič, J. Honkonen, M. Jurčičin, A. Mazzino and S. Sprinc, *Phys. Rev. E* **71**, 066312 (2005).
- [34] E. Jurčičinova and M. Jurčičin, *Phys. Rev. E* **77**, 016306 (2008); E. Jurčičinova, M. Jurčičin and R. Remecky, *Phys. Rev. E* **80**, 046302 (2009).
- [35] E. Jurčičinova, M. Jurčičin, *Phys. Rev. E* **91**, 063009 (2015).
- [36] L. Ts. Adzhemyan, N. V. Antonov, J. Honkonen, and T. L. Kim, *Phys. Rev. E* **71**, 016303 (2005).
- [37] N. V. Antonov, *Phys. Rev. Lett.* **92**, 161101 (2004).
- [38] N. V. Antonov and M. M. Kostenko, *Phys. Rev. E* **90**, 063016 (2014).
- [39] N. V. Antonov, N. M. Gulitskiy, and A. V. Malyshev, *EPJ Web of Conf.* **126**, 04019 (2016).
- [40] E. Jurčičinova, M. Jurčičin, R. Remecky, *Phys. Rev. E* **93**, 033106 (2016).
- [41] T. Elperin, N. Kleeorin, and I. Rogachevskii, *Phys. Rev E* **52**, 2617 (1995); *E* **55** 2713 (1997); *Phys. Rev. Lett.* **76** 224 (1996).
- [42] M. Vergassola and A. Mazzino, *Phys. Rev. Lett.* **79**, 1849 (1997).
- [43] M. Vergassola and M. Avellaneda, *Physica D* **106** 148 (1997).
- [44] A. Celani, A. Lanotte, and A. Mazzino, *Phys. Rev. E* **60** R1138 (1999).
- [45] M. Chertkov, I. Kolokolov, and M. Vergassola, *Phys. Rev. E* **56**, 5483 (1997); *Phys. Rev. Lett.* **80**, 512 (1998).
- [46] K. Gawędzki and M. Vergassola, *Physica D* **138**, 63 (2000).
- [47] L. Ts. Adzhemyan and N. V. Antonov, *Phys. Rev. E* **58**, 7381 (1998).
- [48] N. V. Antonov and J. Honkonen, *Phys. Rev. E* **63**, 036302 (2001).
- [49] N. V. Antonov and P. Gol'din, *Theor. Math. Phys.* **141**, 1725 (2004).
- [50] N. V. Antonov, *Physica D* **144**, 370 (2000).

- [51] M. Hnatich, E. Jurčišínova, M. Jurčišín, and M. Repašan, *J. Phys. A: Math. Gen.* **39**, 8007 (2006).
- [52] V. S. L'vov and A. V. Mikhailov, *Sov. Phys. JETP* **47**, 756 (1978).
- [53] L. Ts. Adzhemyan, M. Yu. Nalimov, and M. M. Stepanova, *Theor. Math. Phys.* **104**, 971 (1995);
N. V. Antonov, M. Hnatich, and M. Yu. Nalimov, *Phys. Rev. E* **60**, 4043 (1999).
- [54] D. Yu. Volchenkov and M. Yu. Nalimov, *Theor. Math. Phys.* **106**, 375 (1996).
- [55] N. V. Antonov, M. Yu. Nalimov and A. A. Udalov, *Theor. Math. Phys.* **110**, 305 (1997).
- [56] I. Staroselsky, V. Yakhot, S. Kida, and S. A. Orszag, *Phys. Rev. Lett.*, **65**, 171 (1990).
- [57] S. S. Moiseev, A. V. Tur, and V. V. Yanovskii, *Sov. Phys. JETP* **44**, 556 (1976).
- [58] J. Honkonen and M. Yu. Nalimov, *Z. Phys. B* **99**, 297 (1996).
- [59] D. Ronis, *Phys. Rev. A* **36**, 3322 (1987); L. Ts. Adzhemyan, J. Honkonen, M. V. Kompaniets, A. N. Vasil'ev, *Phys. Rev. E* **68**, 055302(R) (2003); L. Ts. Adzhemyan, M. Hnatich and J. Honkonen, *Eur. Phys. J B* **73**, 275 (2010).
- [60] L. Ts. Adzhemyan, J. Honkonen, M. V. Kompaniets, and A. N. Vasil'ev, *Phys. Rev. E* **71**, 036305 (2005).
- [61] D. Forster, D.R. Nelson, and M.J. Stephen, *Phys. Rev. Lett.* **36**, 867 (1976); *Phys. Rev. A* **16**, 732 (1977).
- [62] Š. Birnšteinová, M. Hnatič, T. Lučivjanský, and L. Mižišin, in progress.
- [63] N. V. Antonov, N. M. Gulitskiy, M. M. Kostenko, and T. Lučivjanský, *EPJ Web of Conf.* **125**, 05006 (2016).
- [64] L. D. Landau and E. M. Lifshitz, *Fluid Mechanics* (Pergamon Press, Oxford).
- [65] L. Ts. Adzhemyan, N. V. Antonov, M. V. Kompaniets, and A. N. Vasil'ev, *Int. J. Mod. Phys. B* **17**, 2137 (2003).
- [66] C. De Dominicis and P. C. Martin, *Phys. Rev. A* **19**, 419 (1979); J. D. Fournier and U. Frisch, *Phys. Rev. A* **28**, 1000 (1983); L. Ts. Adzhemyan, A. N. Vasil'ev, and Yu. M. Pis'mak, *Theor. Math. Phys.* **57**, 1131 (1983).
- [67] L. Ts. Adzhemyan, A. N. Vasil'ev, and M. Hnatich, *Theor. Math. Phys.* **74**, 115 (1988); L. Ts. Adzhemyan, N. V. Antonov, and T. L. Kim, *Theor. Math. Phys.* **100**, 1086 (1994); N. V. Antonov, S. V. Borisenok, and V. I. Girina, *Theor. Math. Phys.* **106**, 75 (1996); N. V. Antonov and A. N. Vasil'ev, *Theor. Math. Phys.* **110**, 97 (1997).
- [68] B. Duplantier, A. W. W. Ludwig, *Phys. Rev. Lett.* **66**, 247 (1991); G. L. Eyink, *Phys. Lett. A* **172**, 355 (1993).